Check for updates

Comparative evaluation and optimization of microwave and ultrasound assisted extraction of stevia secondary bioactive compounds using RSM and ANN–GA approaches

Prakash Kumar [ID] and Punyadarshini Punam Tripathy [ID] *

The increasing demand for functional foods enriched with bioactive compounds has encouraged the exploration of advanced extraction techniques. *Stevia rebaudiana*, a natural herb rich in bioactive compounds with antioxidant, anti-inflammatory, and anti-diabetic properties, shows considerable potential for functional food applications. This study optimized microwave assisted extraction (MAE) and ultrasound assisted extraction (UAE) to maximize the recovery of stevia's secondary bioactive metabolites. Single-factor analysis revealed that a 50% ethanol concentration at 50 °C significantly ($p < 0.05$) increased the phenolic content by 33.06% compared to water as a solvent. Second-order quadratic models developed using response surface methodology (RSM) showed strong statistical significance ($p < 0.0001$) and high adjusted R^2 values, ranging from 0.8893–0.9533 for MAE and 0.9177–0.9326 for UAE, confirming model reliability. Comparative experimental design analysis indicated that MAE outperformed UAE, yielding 8.07%, 11.34%, and 5.82% higher total phenolic content (TPC), total flavonoid content (TFC), and antioxidant activity (AA), respectively, with 58.33% less extraction time. Artificial neural networks coupled with genetic algorithm (ANN–GA) models further improved predictive accuracy, with the MAE model achieving an R^2 of 0.9985 and a mean squared error (MSE) of 0.7029, outperforming the UAE model (R^2 of 0.9981 and MSE of 0.8362). The ANN–GA predicted optimized MAE conditions of 5.15 min extraction time, 284.05 W microwave power, 53.10% ethanol concentration, and 53.89 °C temperature, yielded higher TPC, TFC, and AA values with minimal error. These results established MAE as a more efficient, sustainable, and effective method for extracting bioactive compounds from stevia leaves compared to UAE.

Sustainability spotlight

Sustainable food processing demands green extraction technologies that maximize the recovery of bioactive compounds while reducing environmental impacts. Conventional methods are both time- and solvent-intensive, often degrading heat-sensitive bioactive compounds. Ultrasound-assisted extraction (UAE) and microwave-assisted extraction (MAE) offer eco-friendly alternatives, enabling rapid, high-yield recovery of stevia's bioactive metabolites through acoustic cavitation and dielectric heating, respectively. These methods minimize solvent and energy use while maintaining the structural and functional integrity of bioactive compounds, thereby supporting global sustainability goals. To further enhance efficiency and scalability, green bioprocessing increasingly employs statistical optimization and machine learning models, such as response surface methodology (RSM) and artificial neural networks integrated with genetic algorithms (ANN–GA).

1 Introduction

The rising prevalence of diet-related health issues has increased awareness of the importance of dietary choices, leading to a growing demand for food products enriched with bioactive compounds that provide both essential nutrients and additional health benefits.[1,2] The secondary metabolites of bioactive compounds, such as polyphenols, terpenoids, alkaloids, and other classes of nitrogen-containing compounds, are known for their strong antioxidant and anti-inflammatory properties.[3] Through their ability to scavenge free radicals, mitigate oxidative stress, and modulate inflammatory pathways, they play a crucial role in reducing the risk of chronic diseases.[4] As a result, functional foods enriched with bioactive compounds have gained considerable attention for their potential to support overall health and well-being.[2,5] This shift in consumer preferences has driven the food industry to focus on developing advanced processing technologies. These technologies are designed to preserve nutritional quality and bioactive

Agricultural and Food Engineering Department, Indian Institute of Technology Kharagpur, Kharagpur, 721302, West Bengal, India. E-mail: punam@agfe.iitkgp.ac. in; Fax: +91 3222 282244; Tel: +91 3222 283174

compounds, while simultaneously ensuring product safety, environmental sustainability, and minimal quality degradation.

Among many sources of bioactive compounds, *Stevia rebaudiana* (stevia) stands out as a promising natural herb with significant therapeutic potential.[1,6,7] As a nutraceutical, stevia is rich in bioactive compounds that support its health-promoting properties.[8] It is considered safe, cost-effective, and widely accessible, making it a preferred alternative to dietary sugar, particularly as a low (or no)-calorie sweetener with a sweetness intensity approximately 250–300 times that of sucrose.[6,8–10] Beyond its sweetening role, stevia leaves contain a diverse spectrum of phytochemicals that enhance its nutraceutical value.[6] These include phenolic compounds such as phenolic acids (chlorogenic, caffeic, ferulic, vanillic, syringic, and iso-chlorogenic acids) and flavonoids (diosmin, rutin, quercetin, kaempferol, luteolin, apigenin, diosmetin, and casticin), which largely contribute to its strong antioxidant potential.[6–8,11–13] In addition, lipids and fatty acids (linolenic, palmitic, oleic, and stearidonic acids), polysaccharides (including inulin-type fructooligosaccharides and oligosaccharides), vitamins (such as folic acid, vitamin C, and vitamin B2), amino acids (L-tyrosine and D-tryptophan), and essential minerals have also been reported.[1,6,8,14] Moreover, stevia offers various potential health benefits, including antioxidant, antimicrobial, and anti-inflammatory effects, as well as the ability to regulate blood sugar and lipids metabolism. These properties, along with possible anti-cancer effects, highlight its potential as a valuable ingredient for future functional foods.[6,15–17]

The extraction of secondary metabolites from stevia has remained challenging for decades, as conventional methods are often time-consuming and inefficient.[12] Hydrodistillation, maceration, and Soxhlet extraction are widely used extraction methods; however, they require extended processing times and, high solvent and energy consumption, and may lead to the degradation of heat-sensitive compounds, reducing their bioactive properties.[18] The yield and quality of these bioactive compounds are heavily influenced by factors such as the extraction method, solvent type, and solvent polarity.[18–20] To overcome these limitations, researchers have explored advanced techniques like supercritical fluid extraction (SFE), subcritical solvent extraction (SSE), pulsed electric field extraction (PEF), pressurized liquid extraction (PLE), ultrasound assisted extraction (UAE), microwave assisted extraction (MAE), and enzyme assisted extraction (EAE).[5,18,19,21] These innovative methods not only improve efficiency and reduce extraction time but also, in some cases, reduce environmental impact while maximizing the recovery of valuable bioactive compounds.

Among these advanced techniques, UAE and MAE have gained significant attention due to their efficiency, eco-friendliness, and ability to preserve bioactive compounds.[5,12,21–23] UAE utilizes acoustic cavitation, where high-frequency sound waves generate microscopic bubbles that collapse, creating localized high temperatures and pressures.[24] This process disrupts plant cell walls, enhancing the release of bioactive compounds into the solvent.[25] On the other hand, MAE applies microwave energy to heat the solvent and plant material through dielectric heating, which accelerates mass transfer and improves extraction yield.[23]

Both techniques offer rapid and effective extraction while minimizing solvent use, energy consumption, and thermal degradation of heat-sensitive compounds. Their ability to optimize extraction efficiency, while maintaining the integrity of bioactive compounds makes UAE and MAE promising green extraction technologies for applications in functional foods and other industries requiring high-quality bioactive extracts.[2,5,19] However, existing comparative analyses of these techniques for stevia leaves are limited, thereby highlighting the significance of the present study in advancing scientific understanding.

To further enhance the optimization of the UAE and MAE processes, response surface methodology (RSM) has been widely applied to model and optimize the extraction conditions.[20] Within RSM, the central composite rotatable design (CCRD) is widely used as it integrates factorial, axial, and center points to ensure efficient coverage and robust modeling with fewer runs than a full factorial design.[20,26,27] While effective in analyzing variable interactions, RSM has inherent limitations in capturing highly complex and non-linear relationships within the process. In contrast, artificial neural networks (ANNs), inspired by biological neural systems, offer a data-driven modeling approach capable of learning intricate, nonlinear dependencies between input and output variables. When coupled with optimization techniques such as genetic algorithm (GA), which mimic evolutionary principles to search for global optima, ANN can significantly improve prediction accuracy and process optimization.[2,26,27] Similarly, integrating RSM with ANN provides a robust framework for precise modeling and prediction, thereby enhancing the efficiency of bioactive compound recovery.[2,28,29]

Due to the limited literature on the simultaneous evaluation of MAE and UAE under the influence of four independent variables (extraction time, temperature, microwave power/ultrasound amplitude, and solvent concentration), this study presents a novel comparative framework. A central composite rotatable design (CCRD) within the response surface methodology (RSM) was first employed to examine the linear and interactive effects of the selected variables. To address the limitations of RSM in modeling nonlinear and complex relationships, an artificial neural network (ANN) coupled with a genetic algorithm (GA) model was developed. This ANN–GA hybrid approach enhanced predictive accuracy and facilitated more efficient optimization of the extraction conditions.

The objectives of this study are:

● To quantify the secondary metabolites, specifically total phenolic content (TPC) and total flavonoid content (TFC), and also evaluate the antioxidant activity (AA) in stevia extracts obtained through MAE and UAE techniques.

● To develop, optimize, and validate RSM and ANN-GA models for predicting the secondary metabolites with minimal error.

2 Materials and methods

2.1 Chemicals and reagents

2,2-Diphenyl-2-picrylhydrazyl (DPPH, 95.0%), aluminum chloride anhydrous powder (AlCl₃, 98%), ethanol (EtOH, 99%), Folin–Ciocalteu reagent (FCR), gallic acid (99.5%), sodium

carbonate anhydrous (Na_2CO_3, 99.0%), sodium hydroxide (NaOH, 97.0%), quercetin (QC, 95%), and sodium nitrite ($NaNO_2$, 98.0%) were procured from Merck Life Science Pvt. Ltd., India.

2.2 Sample preparation

Based on our previous work, Kumar and Tripathy,[30] stevia leaves dried using an indirect mode solar dryer (ISD) with an average leaf temperature of 55.87 ± 1.10 °C were used for the extraction process. The dried leaves were finely ground using a mechanical grinder (Bajaj Rex 500 W, India) and passed through a 60-mesh B.S.S. sieve to achieve a uniform particle size of approximately 250 microns. The resulting powder, with a moisture content of 5.94 ± 0.32% (wet basis), was stored in dark, air-tight polybags in a deep freezer (CFHT405, VOLTAS, India) maintained at −18 °C until further experimentation. A sample-to-solvent ratio of 1 : 10 g mL^{-1} was utilized, following previous studies,[10,18,20,26] as it has been reported to maximize the extraction efficiency of bioactive compounds.

2.3 Single factor at a time (SFAT) experimentation

Evaluating the influence of each parameter on phenolic content was essential for establishing the optimal extraction conditions. In the SFAT study, temperature was initially varied from 30–60 °C in 5 °C increments, while keeping the extraction time fixed at 20 min in distilled water with continuous stirring at 200 rpm. After identifying the temperature that maximized TPC, further experiments were conducted by replacing distilled water with EtOH at varying concentrations (0–100% in 25% increments) under identical extraction conditions. Once the optimal temperature and EtOH concentration were determined, experiments were repeated across the same temperature range to further assess its effect on TPC, using EtOH instead of distilled water, while keeping the extraction time constant. To determine the optimal power range for MAE and the amplitude range for UAE, the values were set between 150 and 450 W and 30–60%, respectively, while maintaining a fixed extraction time of 20 min. Additionally, the influence of extraction time on TPC was investigated for both MAE and UAE by varying the time from 3 to 24 min, while keeping all other parameters constant at their identified optimal values. Once the optimum conditions were identified from these seven experimental plans (as shown in Table S1), the parameter ranges for CCRD were established to enable optimization, improve prediction, and assess non-linear second-order polynomial interactions.

2.4 Experimental design parameters for stevia extraction

2.4.1 MAE experimental procedure. MAE was performed using a NuWav-Uno microwave extraction system (NμTech Analytical Technologies Pvt. Ltd., India), equipped with a digital control interface for precise regulation of extraction time and microwave power. Based upon the SFAT experimentation (maximum recovery), experimental runs were carried out at varying time (X_1: 4–6 min), microwave power (X_2: 250–350 W), solvent concentration (X_3: 45–55%), and temperature (X_4: 45–55 °C). After that, the extracted solution was subjected to

centrifugation at 5000×g for 15 min at 4 °C using an RC 4100F centrifuge (Elektrocraft Pvt. Ltd., India) to separate the supernatant. The supernatant was then carefully collected and filtered through Whatman No. 42 filter paper to eliminate residual particulates. The filtered extracts were transferred to storage containers and stored at −18 °C in a deep freezer until further analysis.

2.4.2 UAE experimental procedure. UAE was performed using an ultrasonic system (PRO650, iGene Labserve Private Limited, India), with a maximum input power of 650 W, using a 6 mm probe operating at a frequency of 20 kHz. Based upon the SFAT experimentation, experimental runs were carried out at varying time (A: 10–14 min), ultrasonic amplitude (B: 35–45%), temperature (C: 45–55 °C), solvent concentration (D: 45–55%). Following UAE treatment, the supernatant was separated and handled similarly to MAE.

2.5 Evaluation of TPC, TFC, and antioxidant activity of the stevia extract

2.5.1 Folin–Ciocalteu reagent (FCR) colorimetric method. TPC in the stevia extract was determined using the FCR method, as described in our previous work.[30] The absorbance of the extract was measured at 760 nm using a UV-vis spectrophotometer (UV-2602, LABOMED INC., USA). Gallic acid at a concentration of 0.1 mg mL^{-1} was used as the standard, and TPC was expressed as mg of gallic acid equivalent per gram of dry weight of the stevia sample (mg GAE per g sample).

2.5.2 Aluminum chloride ($AlCl_3$) colorimetric method. TFC was determined using the $AlCl_3$ colorimetric method, as described in our previous work.[30] The absorbance of the incubated extract was measured at 510 nm using a UV-vis spectrophotometer. Quercetin at a concentration of 0.01 mg mL^{-1} was used as the standard and TFC was measured in mg of quercetin equivalent per gram of dry weight of the sample (mg QE per g sample).

2.5.3 Antioxidant activity. The antioxidant activity of the stevia extract was evaluated using the DPPH radical scavenging assay, following the method described by Ali *et al.*[31] with slight modifications. A reaction mixture was prepared by adding 0.2 mL of diluted ethanolic extract to 0.95 mL of freshly prepared DPPH solution and 2.85 mL of EtOH. The mixture was then incubated in the dark at 28 °C for 30 min to ensure complete reaction. After incubation, the absorbance was measured at 517 nm using a UV-vis spectrophotometer. The percentage inhibition of DPPH radicals was calculated using the following eqn (1):

$$\text{Antioxidant activity (AA, \%)} = \left(\frac{\text{Ab}_c - \text{Ab}_{se}}{\text{Ab}_c}\right) \times 100 \quad (1)$$

where Ab_c and Ab_{se} represent the absorbance of the control and stevia extract, respectively.

2.6 Experimental design using RSM

MAE and UAE were systematically compared under the influence of four independent variables. A CCRD with five levels (−α, −1, 0, +1, +α) was employed within the RSM framework to

Table 1 Experimental range of coded values for the central composite rotatable design (CCRD) in response surface methodology (RSM)[a]

Symbol	Independent variables	Units	Coded variable ranges				
For MAE			-2 (or $-\alpha$)	-1	0	$+1$	$+2$ (or $+\alpha$)
X_1	Time	min	3	4	5	6	7
X_2	Power	W	200	250	300	350	400
X_2	Solvent concentration	%	40	45	50	55	60
X_4	Temperature	°C	40	45	50	55	60
For UAE							
A	Time	min	8	10	12	14	16
B	Amplitude	%	30	35	40	45	50
C	Solvent concentration	%	40	45	50	55	60
D	Temperature	°C	40	45	50	55	60

[a] Here, MAE represents microwave assisted extraction and UAE denotes ultrasound assisted extraction.

evaluate the effects and second-order interactions of these variables (as shown in Table 1). Statistical modeling, prediction, and optimization were performed using Design Expert 13 (Stat-Ease Inc., Minneapolis, USA).

2.7 ANN and ANN–GA modeling

The experimental data obtained from MAE and UAE, following the CCRD, were used to train the neural network in MATLAB R2014a (MathWorks, Inc., MA, USA). The neural network design process involved data collection, network creation, configuration, weight and bias initialization, training, validation, and testing. A multilayer perceptron (MLP) network architecture was implemented, consisting of three layers: input, hidden, and output, where independent variables formed the input layer, and three response variables were assigned as the output layer (as shown in Table 1 and Fig. 7(a)). The feedforward process involved propagating the input data through the network, passing through the hidden layers, and computing the output predictions. To ensure reproducibility, the random seed was set using rng('default'); before model training, ensuring consistent initialization of network weights and biases across different runs. For validation and testing, 90 data points were split into training (80%), validation (10%), and testing (10%). To optimize the model, hidden layer sizes of 7–10 neurons were tested, with L2 regularization ($\lambda = 0.10$) was applied to prevent overfitting. The model was trained using a feedforward network with the Levenberg–Marquardt backpropagation (trainlm) algorithm for up to 1000 cycles, minimizing the mean squared error (MSE) between predicted and actual values. The backpropagation process adjusted the network weights by computing the gradient of the error with respect to each weight and updating them in the direction that minimized the loss function. The hyperbolic tangent sigmoid (tansig) transfer function was applied in the hidden layer to introduce non-linearity in feature extraction. However, the linear (purelin) transfer function was used in the output layer to ensure a direct mapping between the network output and target values (as shown in Fig. 7(a)). Early stopping was applied when test performance dropped below 0.5, in order to improve computational efficiency with

unnecessary training. A genetic algorithm (GA) was employed to optimize key hyperparameters, including the number of hidden neurons and the learning rate. It was also used to determine the optimal connection weights and bias values by selecting an appropriate population size, defining the number of genetic generations, and designing a fitness function to enhance model performance. The final integrated ANN model was selected based on the lowest MSE and the highest correlation coefficient (R), ensuring optimal predictive accuracy.

2.8 Statistical analysis

The effectiveness of the applied modeling techniques, including the RSM and ANN model, was evaluated using statistical performance metrics such as the coefficient of determination (R^2), adjusted R^2, MSE, root mean squared error (RMSE), mean absolute deviation (MAD), and mean absolute percentage error (MAPE), as reported by Kumar and Tripathy[30] and mentioned in eqn (2)–(6). The analysis was conducted using MATLAB R2014a (MathWorks, Inc., MA, USA) for ANN-based modeling, Design Expert13 for RSM predictions, Microsoft Excel 2019 (Microsoft Corporation, Redmond, WA, USA), and OriginPro 2021 (OriginLab Corporation, Northampton, MA, USA) for statistical computations and validation.

$$\text{MSE} = \frac{1}{N} \sum_{i=1}^{N} \left(Y_{\text{exp},i} - \hat{Y}_{\text{pre},i} \right)^2 \quad (2)$$

$$\text{RMSE} = \left[\frac{1}{N} \sum_{i=1}^{N} \left(Y_{\text{exp},i} - \hat{Y}_{\text{pre},i} \right)^2 \right]^{1/2} \quad (3)$$

$$\text{MAD} = \frac{1}{N} \sum_{i=1}^{N} \left| \left(Y_{\text{exp},i} - \hat{Y}_{\text{pre},i} \right) \right| \quad (4)$$

$$R^2 = 1 - \left[\frac{\sum_{i=1}^{N} \left(Y_{\text{exp},i} - \hat{Y}_{\text{pre},i} \right)^2}{\sum_{i=1}^{N} \left(Y_{\text{exp},i} - \overline{Y}_{\text{exp},i} \right)^2} \right] \quad (5)$$

$$\text{Adjusted } R^2 = \left[1 - \frac{(1 - R^2)(N - 1)}{(N - z - 1)}\right] \qquad (6)$$

where, N, $Y_{\exp,i}$, $\hat{Y}_{\mathrm{pre},i}$, $\bar{Y}_{\exp,i}$, and z represents the number of experimental runs, the experimental value of the ith run, the predicted value of the ith run, the average of experimental values, and the number of model parameters, respectively.

3 Results and discussion

3.1 Single factor at a time (SFAT) experimental analysis

3.1.1 Effect of the solvent type and temperature on TPC extraction.
Table S1 presents the results of SFAT experiments conducted to determine the optimal conditions for extracting TPC from stevia extract. These data were used to select the parameter ranges for further optimization using CCRD in RSM. Table S1 is divided into seven experimental plans, each investigating the effect of a specific parameter on TPC extraction. In the first experimental plan, it was found that TPC increased significantly ($p < 0.05$) with temperature up to 50 °C when using distilled water (as the solvent), reaching a maximum of 42.94 ± 0.42 mg GAE per g sample. However, beyond 50 °C, TPC declined, indicating potential degradation of phenolic compounds at higher temperatures. In the second experimental plan, EtOH concentration was varied from 0–100% while maintaining a fixed temperature of 50 °C. TPC significantly increased ($p < 0.05$) with rising EtOH concentration, reaching an optimal value of 54.04 ± 0.52 mg GAE per g sample at 50%. Beyond this point, higher EtOH concentrations led to a slight decline in TPC, indicating that 50% EtOH is both optimal and economical for extraction. Similarly, Carbonell-Capella et al.[32] observed a 20.28% increase in TPC at 50% EtOH concentration, attributed to enhanced mass transfer between the solvent and solid phase resulting from increased permeability of plant tissues. In the third experimental plan, the effect of temperature was analyzed at the optimal solvent concentration for phenolic compound extraction. It was found that TPC significantly increased ($p < 0.05$) up to 57.14 ± 0.72 mg GAE per g sample at 50 °C. Beyond this temperature, TPC declined, similar to the trend observed with distilled water extraction. This suggests that while high temperatures have the potential to improve mass transport and disturb the plant matrix, they also raise the possibility of thermal damage.[20,33] Similarly, Che Sulaiman et al.[20] reported the highest phenolic yield from *Clinacanthus nutans* Lindau leaves at 60 °C, with a significant decline observed beyond 80 °C. In conclusion, the SFAT plan showed that ethanolic extraction at 50 °C yielded 25.85% more TPC than water extraction. The fourth to seventh experimental plans are discussed in the following subsections for more clarity.

3.1.2 Effect of microwave power and time on TPC extraction during MAE.
Based on the first three experimental plans, the temperature and EtOH extraction conditions were fixed for subsequent experiments. In the fourth experimental plan (Table S1), the effect of microwave power on TPC was analyzed, showing a significant increase ($p < 0.05$) up to 61.69 ± 0.33 mg GAE per g sample at 300 W, followed by a decline at higher power levels due to temperature induced degradation.

Following these findings, the fifth experimental plan examined the effect of extraction time under optimized conditions (50% EtOH concentration, 50 °C, and 300 W), revealing that TPC increased with time, reaching a maximum of 66.95 ± 0.36 mg GAE per g sample at 6 min. However, a significant ($p < 0.05$) decline was observed beyond 300 W, suggesting that prolonged microwave exposure may lead to degradation or polymerization of phenolic compounds.[34] Bin Mokaizh et al.[22] reported a reduction in bioactive compound recovery above 50 °C when microwave power exceeded 400 W, indicating that higher power inputs may induce carbonization of the plant material. A similar trend was observed in MAE of phenolic compounds from *Euphorbia hirta* leaves, where morphological alterations and reduced thermal stability were evident under elevated processing conditions.[35]

3.1.3 Effect of ultrasonic amplitude and time on TPC extraction during UAE.
In the sixth experimental plan (Table S1), the effect of ultrasonic amplitude on TPC was analyzed under the previously optimized conditions. The results showed that TPC increased with amplitude, reaching a maximum of 58.92 ± 0.56 mg GAE per g sample at 45% amplitude. However, further increases in amplitude led to a significant ($p < 0.05$) decline in TPC, likely due to excessive cavitation effects. Similarly, in the seventh experimental plan, the effect of extraction time on TPC was analyzed under optimized UAE conditions (50% EtOH, 50 °C, and 45% amplitude). The results revealed that TPC increased with time, reaching a maximum of 62.47 ± 0.48 mg GAE per g sample at 10 min. However, prolonged extraction led to a significant decline in TPC, likely due to extended ultrasonic exposure or polymerization.[20,23,24]

3.1.4 Selection of parameter ranges for CCRD in RSM based on SFAT.
CCRD was employed to evaluate factorial points beyond the defined factor levels by incorporating axial ($\pm\alpha$) points, allowing for a more comprehensive analysis of nonlinearity. Based on the SFAT experimental plan, the analysis determined that the optimal ranges for significant TPC extraction were 45–55 °C for temperature and 45–55% for EtOH concentration. For MAE, the selected ranges for further optimization were 4–6 min for extraction time and 250–350 W for microwave power. Similarly, for UAE, the chosen ranges were 10–14 min for extraction time and 35–45% for ultrasonic amplitude (Table S1). These ranges were further optimized using CCRD in RSM for TPC, TFC, and AA of stevia extract.

3.2 RSM modeling: 3D surface analysis and interaction effects of parameters

3.2.1 Model fitting and adequacy for both MAE and UAE extraction techniques.
The response data for MAE and UAE, presented in Table 2 and 3, respectively, were used to develop second-order quadratic models. These models were constructed using multiple regression analysis within the CCRD framework of RSM, incorporating five levels of coded variables (as detailed in Table 1) to evaluate model adequacy, statistical significance, and predictive accuracy. The statistical significance and overall adequacy of the models were evaluated using ANOVA, as presented in Table 4 and 5. The final predictive equations were

Table 2 Design of experiments (DoE) using CCRD to analyze the responses of independent variables in stevia extract obtained through MAE[a]

Standard order	Run	X_1 Time (min)	X_2 Power (W)	X_3 Solvent concentration (%)	X_4 Temperature (°C)	TPC (mg GAE per g sample) Experimental	RSM predicted	ANN predicted	TFC (mg QE per g sample) Experimental	RSM predicted	ANN predicted	AA (%) Experimental	RSM predicted	ANN predicted
21	1	5 (0)	300 (0)	40 (−2)	50 (0)	55.73 ± 0.55	54.6	55.32	21.04 ± 0.15	20.52	20.42	65.03 ± 0.09	64.14	65.27
15	2	4 (−1)	350 (+1)	55 (+1)	55 (+1)	62.90 ± 0.57	63.31	62.72	26.52 ± 0.07	26.23	26.25	91.70 ± 0.06	88.04	91.87
6	3	6 (+1)	250 (−1)	55 (+1)	45 (−1)	59.97 ± 0.40	60.69	60.30	25.27 ± 0.23	24.79	23.52	69.53 ± 0.08	68	69.46
4	4	6 (+1)	350 (+1)	45 (−1)	45 (−1)	59.28 ± 0.36	60.88	59.26	22.93 ± 0.16	23.72	23.52	78.83 ± 0.14	78.34	78.68
11	5	4 (−1)	350 (+1)	45 (−1)	55 (+1)	59.04 ± 0.40	59.4	60.15	23.16 ± 0.21	24.13	22.68	66.00 ± 0.02	68.45	66.03
17	6	3 (−2)	300 (0)	50 (0)	50 (0)	65.78 ± 0.73	64.01	64.41	26.04 ± 0.08	25.46	26.34	65.83 ± 0.06	65.64	65.34
18	7	7 (+2)	300 (0)	50 (0)	50 (0)	65.54 ± 0.36	66.87	66.02	26.56 ± 0.27	26.84	27.94	78.03 ± 0.05	76.93	78.16
5	8	4 (−1)	250 (−1)	55 (+1)	45 (−1)	59.04 ± 0.64	58.59	58.04	21.65 ± 0.21	22	22.25	67.57 ± 0.08	65.8	66.89
14	9	6 (+1)	250 (−1)	55 (+1)	55 (+1)	64.28 ± 0.32	63.29	62.98	25.21 ± 0.21	25.55	25.52	81.37 ± 0.11	83.59	81.80
3	10	4 (−1)	350 (+1)	45 (−1)	45 (−1)	58.23 ± 0.51	58.59	58.01	23.26 ± 0.15	22.74	23.05	72.43 ± 0.07	70.6	72.18
9	11	4 (−1)	250 (−1)	45 (−1)	55 (+1)	56.85 ± 0.15	58.12	58.32	22.30 ± 0.31	22.94	21.69	61.33 ± 0.11	63.8	61.65
1	12	4 (−1)	250 (−1)	45 (−1)	45 (−1)	56.56 ± 0.36	57.47	56.36	20.52 ± 0.11	20.54	21.38	64.10 ± 0.06	62.1	63.95
26	13	5 (0)	300 (0)	50 (0)	50 (0)	68.26 ± 0.43	67.42	67.40	30.42 ± 0.11	30.91	30.79	95.30 ± 0.05	92.47	92.57
27	14	5 (0)	300 (0)	50 (0)	50 (0)	67.81 ± 0.39	67.42	67.40	30.51 ± 0.11	30.91	30.79	93.87 ± 0.04	92.47	92.57
20	15	5 (0)	400 (+2)	50 (0)	50 (0)	61.85 ± 0.69	60.85	60.85	24.37 ± 0.22	24.19	25.28	85.17 ± 0.10	83.78	84.49
12	16	6 (+1)	350 (+1)	45 (−1)	55 (+1)	60.35 ± 0.65	60.16	60.39	23.25 ± 0.19	22.72	23.42	75.40 ± 0.07	77.55	75.69
2	17	6 (+1)	250 (−1)	45 (−1)	45 (−1)	58.73 ± 0.36	57.68	58.30	21.33 ± 0.08	21.43	21.56	62.77 ± 0.10	66.81	62.96
28	18	5 (0)	300 (0)	50 (0)	50 (0)	66.50 ± 0.50	67.42	67.40	29.93 ± 0.12	30.91	30.79	85.40 ± 0.03	92.47	92.57
8	19	6 (+1)	350 (+1)	55 (+1)	45 (−1)	65.12 ± 0.43	63.21	64.88	27.79 ± 0.08	26.97	27.31	84.97 ± 0.05	82.88	85.02
22	20	5 (0)	300 (0)	60 (+2)	50 (0)	60.83 ± 0.38	61.51	62.43	25.77 ± 0.08	25.98	25.33	85.33 ± 0.04	84.92	84.74
25	21	5 (0)	300 (0)	50 (0)	50 (0)	67.69 ± 0.33	67.42	67.40	31.97 ± 0.15	30.91	30.79	93.57 ± 0.09	92.47	92.57
13	22	4 (−1)	250 (−1)	55 (+1)	55 (+1)	63.23 ± 0.50	62.71	63.26	25.46 ± 0.07	25.16	25.95	78.63 ± 0.10	80.04	79.04
19	23	5 (0)	200 (−2)	50 (0)	50 (0)	56.49 ± 0.47	57.05	57.03	20.94 ± 0.18	20.82	21.33	64.17 ± 0.02	64.25	64.71
7	24	4 (−1)	350 (+1)	55 (+1)	45 (−1)	57.40 ± 0.61	59.04	58.87	23.47 ± 0.15	24.08	23.38	73.03 ± 0.05	77.65	72.82
30	25	5 (0)	300 (0)	50 (0)	50 (0)	66.16 ± 0.61	67.42	67.40	31.12 ± 0.17	30.91	30.79	93.13 ± 0.09	92.47	92.57
16	26	6 (+1)	350 (+1)	55 (+1)	55 (+1)	65.78 ± 0.86	65.96	65.08	26.25 ± 0.24	26.72	26.82	91.70 ± 0.07	94.62	91.94
29	27	5 (0)	300 (0)	50 (0)	50 (0)	68.12 ± 0.54	67.42	67.40	31.54 ± 0.11	30.91	30.79	93.57 ± 0.11	92.47	92.57
24	28	5 (0)	300 (0)	50 (0)	60 (+2)	60.49 ± 0.54	60.74	61.04	24.91 ± 0.24	24.47	24.57	88.90 ± 0.06	86.42	90.01
23	29	5 (0)	300 (0)	50 (0)	40 (−2)	58.02 ± 0.56	57.33	58.24	22.19 ± 0.11	22.32	22.43	71.80 ± 0.07	72.98	71.75
10	30	6 (+1)	250 (−1)	45 (−1)	55 (+1)	57.37 ± 0.47	56.81	56.81	21.56 ± 0.15	21.44	21.59	73.57 ± 0.04	69.86	73.28

[a] Note: TPC represents the total phenolic content (mg GAE per g sample), TFC denotes the total flavonoid content (mg QE per g sample), and AA refers to the antioxidant activity or inhibition (%). QE refers to quercetin equivalent, and GAE signifies gallic acid equivalent.

Table 3 Design of experiments (DoE) using CCRD to analyze the responses of independent variables in stevia extract obtained through UAE[a]

| Standard order | Run | Independent variables | | | | TPC (mg GAE per g sample) | | | TFC (mg QE per g sample) | | | AA (%) | | |
		A Time (min)	B Amplitude (%)	C Solvent concentration (%)	D Temperature (°C)	Experimental	RSM predicted	ANN predicted	Experimental	RSM predicted	ANN predicted	Experimental	RSM predicted	ANN predicted
28	1	12 (0)	40 (0)	50 (0)	50 (0)	61.85 ± 0.22	62.01	61.72	28.14 ± 1.00	27.78	27.64	89.67 ± 0.05	88.67	88.49
16	2	14 (+1)	45 (+1)	55 (+1)	55 (+1)	58.92 ± 0.29	58.8	58.87	27.21 ± 0.81	26.96	26.56	84.20 ± 0.06	86.83	84.03
9	3	10 (−1)	35 (−1)	45 (−1)	55 (+1)	50.20 ± 0.44	51.77	50.36	19.57 ± 0.26	19.79	20.23	71.67 ± 0.06	69.99	71.59
29	4	12 (0)	40 (0)	50 (0)	50 (0)	62.76 ± 1.43	62.01	61.72	27.92 ± 0.95	27.78	27.64	89.27 ± 0.03	88.67	88.49
26	5	12 (0)	40 (0)	50 (0)	50 (0)	63.16 ± 1.58	62.01	61.72	27.12 ± 2.00	27.78	27.64	84.77 ± 0.07	88.67	88.49
13	6	10 (−1)	35 (−1)	55 (+1)	55 (+1)	53.49 ± 0.65	52.35	54.25	24.71 ± 1.25	24.02	24.26	78.87 ± 0.01	78.21	78.32
8	7	14 (+1)	45 (+1)	55 (+1)	45 (−1)	57.25 ± 0.47	56.15	57.39	26.11 ± 2.21	25.48	27.04	83.10 ± 0.03	83.56	82.77
22	8	12 (0)	40 (0)	60 (+2)	50 (0)	53.25 ± 0.47	54.31	53.65	24.34 ± 0.43	25.39	25.22	79.99 ± 0.08	80.77	79.77
19	9	12 (0)	30 (−2)	50 (0)	50 (0)	46.10 ± 0.64	47.10	46.31	18.47 ± 0.64	19.52	18.67	57.83 ± 0.05	62.19	58.26
3	10	10 (−1)	45 (+1)	45 (−1)	45 (−1)	49.13 ± 0.25	49.59	49.93	20.87 ± 0.20	20.41	21.15	64.80 ± 0.05	63.83	64.72
5	11	10 (−1)	35 (−1)	55 (+1)	45 (−1)	49.99 ± 0.48	48.84	50.29	21.18 ± 0.19	20.42	21.08	65.97 ± 0.06	64.35	65.73
10	12	14 (+1)	35 (−1)	45 (−1)	55 (+1)	50.96 ± 0.54	49.46	51.14	21.41 ± 0.23	20.05	20.82	67.00 ± 0.06	63.89	67.04
7	13	10 (−1)	45 (+1)	55 (+1)	45 (−1)	48.84 ± 0.51	50.15	48.53	21.77 ± 0.18	22.38	21.38	67.93 ± 0.08	69.58	67.90
12	14	14 (+1)	45 (+1)	45 (−1)	55 (+1)	51.44 ± 0.60	53.05	51.38	22.10 ± 0.12	22.45	21.37	68.70 ± 0.09	69.09	68.51
20	15	12 (0)	50 (+2)	50 (0)	50 (0)	53.25 ± 0.33	51.99	53.03	23.76 ± 0.23	23.87	24.18	74.30 ± 0.01	72.62	74.27
15	16	10 (−1)	45 (+1)	55 (+1)	55 (+1)	54.09 ± 0.44	54.22	54.09	24.67 ± 0.82	23.78	24.46	78.18 ± 0.11	74.34	77.79
4	17	14 (+1)	45 (+1)	45 (−1)	45 (−1)	50.20 ± 0.29	51.14	50.17	23.04 ± 0.15	22.98	22.60	72.20 ± 0.06	71.40	72.26
2	18	14 (+1)	35 (−1)	45 (−1)	45 (−1)	47.77 ± 0.44	48.11	48.08	17.91 ± 0.16	18.39	17.30	54.47 ± 0.09	57.09	54.46
23	19	12 (0)	40 (0)	50 (0)	40 (−2)	50.27 ± 0.48	49.93	50.04	20.06 ± 0.20	20.49	20.38	66.73 ± 0.05	68.08	67.03
30	20	12 (0)	40 (0)	50 (0)	50 (0)	62.26 ± 0.50	62.01	61.72	28.71 ± 0.70	27.78	27.64	89.80 ± 0.04	88.67	88.49
25	21	12 (0)	40 (0)	50 (0)	50 (0)	60.45 ± 3.82	62.01	61.72	27.21 ± 0.40	27.78	27.64	88.47 ± 0.09	88.67	88.49
27	22	12 (0)	40 (0)	50 (0)	50 (0)	61.57 ± 3.60	62.01	61.72	27.57 ± 0.67	27.78	27.64	90.07 ± 0.02	88.67	88.49
21	23	12 (0)	40 (0)	40 (−2)	50 (0)	50.04 ± 0.56	48.72	49.91	18.54 ± 0.22	18.66	18.94	58.50 ± 0.11	60.39	58.57
24	24	12 (0)	40 (0)	50 (0)	60 (+2)	55.28 ± 0.72	55.35	55.50	22.84 ± 0.89	23.57	23.42	78.30 ± 0.04	79.63	77.64
6	25	14 (+1)	35 (−1)	55 (+1)	45 (−1)	52.16 ± 0.74	52.39	52.42	21.85 ± 0.20	21.15	22.34	68.77 ± 0.10	66.14	68.42
17	26	8 (−2)	40 (0)	50 (0)	50 (0)	52.78 ± 0.50	52.57	52.30	19.66 ± 0.25	20.34	19.29	60.93 ± 0.05	64.61	62.00
11	27	10 (−1)	45 (+1)	45 (−1)	55 (+1)	53.35 ± 0.62	52.91	52.97	19.87 ± 0.15	19.81	19.83	61.83 ± 0.06	63.00	61.85
18	28	16 (+2)	40 (0)	50 (0)	50 (0)	56.30 ± 0.34	56.25	56.55	23.23 ± 0.11	23.71	23.73	73.50 ± 0.08	72.49	73.26
14	29	14 (+1)	35 (−1)	55 (+1)	55 (+1)	54.49 ± 0.54	54.49	54.10	24.78 ± 1.35	24.83	25.42	78.77 ± 0.07	78.52	78.41
1	30	10 (−1)	35 (−1)	45 (−1)	45 (−1)	49.08 ± 0.42	49.01	48.86	18.70 ± 0.19	18.20	18.76	65.80 ± 0.12	61.71	66.34

[a] Here, TPC represents the total phenolic content (mg GAE per g sample), TFC denotes the total flavonoid content (mg QE per g sample), and AA refers to the antioxidant activity or inhibition (%). QE refers to quercetin equivalent, and GAE signifies gallic acid equivalent.

Table 4 Quadratic model coefficients and ANOVA results for microwave assisted extraction (MAE) of dried stevia leaf extract[a]

MAE of stevia leaf extract

Model parameters	Coefficient	TPC	TFC	AA
Intercept	β_0	-401.8392***	-483.5334***	-788.8028***
Model				
X_1-time (min)	β_1	$+1.6656$*	$+13.3695$*	$+54.1611$**
X_2-power (W)	β_2	$+0.5018$**	$+0.5753$***	$+1.1542$***
X_3-solvent concentration (%)	β_3	$+7.7123$***	$+7.1202$***	$+12.3353$***
X_4-temperature (°C)	β_4	$+7.1616$**	$+8.1527$**	$+7.9953$***
Interaction				
$X_1 \times X_2$	β_{12}	$+0.0104$	$+0.0005$	$+0.0152$
$X_1 \times X_3$	β_{13}	$+0.0941$	$+0.0951$*	-0.1258
$X_1 \times X_4$	β_{14}	-0.0762	-0.1199**	$+0.0675$
$X_2 \times X_3$	β_{23}	-0.0007	-0.0001	$+0.0034$
$X_2 \times X_4$	β_{24}	$+0.0002$	-0.0010	-0.0039
$X_3 \times X_4$	β_{34}	$+0.0347$*	$+0.0075$	$+0.1253$**
Second order				
X_1^2	β_{11}	-0.4953	-1.1920***	-5.2972***
X_2^2	β_{22}	-0.0009***	-0.0008***	-0.0018***
X_3^2	β_{33}	-0.0937***	-0.0766***	-0.1794***
X_4^2	β_{44}	-0.0839***	-0.0752***	-0.1277***
R^2		0.9428	0.9758	0.9480
Adjusted R^2		0.8893	0.9533	0.8994
Predicted R^2		0.7048	0.8971	0.7751
p-Value		<0.0001***	<0.0001***	<0.0001***
F Value		17.65	43.27	19.53
Lack of fit		0.1126	0.5664	0.5331

[a] Here, TPC represents the total phenolic content (mg GAE per g sample), TFC denotes the total flavonoid content (mg QE per g sample), and AA refers to the antioxidant activity or inhibition (%). QE refers to quercetin equivalent, and GAE signifies gallic acid equivalent. Significance levels: *p < 0.05, **p < 0.01, and ***p < 0.001. Model equation: $Y_{(1,(TPC \text{ or } TFC \text{ or } AA))} = \beta_0 + \beta_1 X_1 + \beta_2 X_2 + \beta_3 X_3 + \beta_4 X_4 + \beta_{12}(X_1 \times X_2) + \beta_{13}(X_1 \times X_3) + \beta_{14}(X_1 \times X_4) + \beta_{23}(X_2 \times X_3) + \beta_{24}(X_2 \times X_4) + \beta_{34}(X_3 \times X_4) + \beta_{11}X_1^2 + \beta_{22}X_2^2 + \beta_{33}X_3^2 + \beta_{44}X_4^2$.

derived from the regression coefficients of the target responses. These models demonstrated strong statistical significance, confirmed by highly significant p-values (p < 0.0001) and F-values ranging from 17.6479 to 43.2707 for MAE (as shown in Table S2–S4) and 24.1014 to 29.6698 for UAE (as shown in Table S5–S7). These results confirm the adequacy of the developed models and their reliable predictive capability. Model performance was further evaluated using multiple goodness-of-fit metrics. The coefficient of determination (R^2) values were 0.9522–0.9801 for MAE (as shown in Fig. S1) and 0.9574–0.9651 for UAE (as shown in Fig. S2), demonstrating a strong correlation between predicted and experimental values. The adjusted R^2 values, which account for the number of predictors, were 0.8893–0.9533 for MAE and 0.9177–0.9326 for UAE, confirming the model's ability to explain a substantial proportion of the observed variance while minimizing the risk of overfitting. Furthermore, the predicted R^2 values, which assess the model's predictive reliability, ranged from 0.7048 to 0.8971 for MAE and 0.7813 to 0.8276 for UAE, indicating strong predictive performance and consistency with experimental data. The lack-of-fit confirmed the adequacy of the quadratic models, as all responses exhibited statistically non-significant p-values (p > 0.05), indicating no significant discrepancy between the

predicted and experimental values. Specifically, for MAE, the lack-of-fit p-values were 0.1126 for TPC, 0.5664 for TFC, and 0.5331 for AA, while for UAE, the corresponding values were 0.2048, 0.1495, and 0.1206, respectively. These results suggested that the models accurately represent the experimental data without systematic bias.

Tables 4 and S2–S4 present the statistical analysis of MAE, revealing that the independent variables exhibited distinct significance patterns across the response variables. Ethanol concentration (X_3) showed the highest significance (p < 0.0001) for TPC, TFC, and AA due to its dual role in optimizing solvent polarity for polyphenol solubility and facilitating cell wall disruption through hydrogen bond formation. Extraction time (X_1) demonstrated a greater impact on AA (p < 0.0001) compared to TPC (p = 0.0208) or TFC (p = 0.0390), reflecting the kinetic requirements of antioxidant extraction, where sufficient time is needed for thermolabile antioxidant release but excessive exposure risks phenolic degradation. Microwave power (X_2) exerted a more significant effect on AA and TFC (p < 0.0001) than on TPC (p = 0.0037), as flavonoids and antioxidants exhibited greater thermal and dielectric susceptibility, facilitating enhanced cell disruption and improved mass transfer during extraction.[36] Most notably, temperature (X_4) showed

Table 5 Quadratic model coefficients and ANOVA results for ultrasound assisted extraction (UAE) of dried stevia leaf extract[a]

UAE of stevia leaf extract

Model parameters	Coefficient	TPC	TFC	AA
Intercept	β'_0	−626.0202***	−408.2041***	−1128.2389***
Linear terms				
A-Time (min)	β'_1	+5.6163**	+5.9028***	+12.8208**
B-Power (W)	β'_2	+8.8415***	+5.5969***	+16.8781***
C-Solvent concentration (%)	β'_3	+8.7792***	+5.0305***	+13.1541***
D-Temperature (°C)	β'_4	+9.4641***	+5.7492***	+16.6926***
Interaction				
$A \times B$	β'_{12}	+0.0611	+0.0593*	+0.3047**
$A \times C$	β'_{13}	+0.1112**	+0.0135	+0.1600
$A \times D$	β'_{14}	−0.0353	+0.0019	−0.0370
$B \times C$	β'_{23}	−0.0072	−0.0026	+0.0311
$B \times D$	β'_{24}	+0.0055	−0.0219*	−0.0911**
$C \times D$	β'_{34}	+0.0074	+0.0201*	+0.0558
Second order				
A^2	β'_{11}	−0.4750***	−0.3595***	−1.2574***
B^2	β'_{22}	−0.1246***	−0.0608***	−0.2127***
C^2	β'_{33}	−0.1049***	−0.0576***	−0.1809***
D^2	β'_{44}	−0.0936***	−0.0575***	−0.1482***
R^2		0.9651	0.9643	0.9574
Adjusted R^2		0.9326	0.9310	0.9177
Predicted R^2		0.8276	0.8191	0.7813
p-Value		<0.0001***	<0.0001***	<0.0001***
F Value		29.6698	28.9515	24.1014
Lack of fit		0.2048	0.1495	0.1206

[a] Here, TPC represents the total phenolic content (mg GAE per g sample), TFC denotes the total flavonoid content (mg QE per g sample), and AA refers to the antioxidant activity or inhibition (%). QE refers to quercetin equivalent, and GAE signifies gallic acid equivalent. Significance levels: *p < 0.05, **p < 0.01, and ***p < 0.001. Model equation: $Y_{(2,(\text{TPC or TFC or AA}))} = \beta'_0 + \beta'_1 A + \beta'_2 B + \beta'_3 C + \beta'_4 D + \beta'_{12}(A \times B) + \beta'_{13}(A \times C) + \beta'_{14}(A \times D) + \beta'_{23}(B \times C) + \beta'_{24}(B \times D) + \beta'_{34}(C \times D) + \beta'_{11}(A^2) + \beta'_{22}(B^2) + \beta'_{33}(C^2) + \beta'_{44}(D^2)$.

exceptional significance for AA (p = 0.0003) relative to TPC (p = 0.0077) and TFC (p = 0.0030), directly reflecting AA's noticeable temperature sensitivity, where optimal thermal conditions are crucial for both antioxidant compound stability and activity preservation, while moderately elevated temperatures suffice for phenolic compound extraction. The second-order polynomial regression models derived from the MAE process are shown in eqn (7)–(9).

$$
\begin{aligned}
Y_{(1,\text{TPC})} \text{ (mg GAE per g sample)} = {} & -401.8392 \\
& + 1.6656 X_1 + 0.5018 X_2 + 7.7123 X_3 \\
& + 7.1616 X_4 + 0.0104 X_1 X_2 + 0.0941 X_1 X_3 \\
& - 0.0762 X_1 X_4 - 0.0007 X_2 X_3 + 0.0002 X_2 X_4 \\
& + 0.0347 X_3 X_4 - 0.4953 X_1^2 - 0.0009 X_2^2 \\
& - 0.0937 X_3^2 - 0.0839 X_4^2
\end{aligned} \tag{7}
$$

$$
\begin{aligned}
Y_{(1,\text{TFC})} \text{ (mg QE per g sample)} = {} & -483.5334 \\
& + 13.3695 X_1 + 0.5753 X_2 + 7.1202 X_3 \\
& + 8.1527 X_4 + 0.0005 X_1 X_2 + 0.0951 X_1 X_3 \\
& - 0.1199 X_1 X_4 - 0.0001 X_2 X_3 - 0.0010 X_2 X_4
\end{aligned}
$$

$$
\begin{aligned}
& + 0.0075 X_3 X_4 - 1.1920 X_1^2 - 0.0008 X_2^2 \\
& - 0.0766 X_3^2 - 0.0752 X_4^2
\end{aligned} \tag{8}
$$

$$
\begin{aligned}
Y_{(1,\text{AA})}(\%) = {} & -788.8028 + 54.1611 X_1 + 1.1542 X_2 \\
& + 12.3353 X_3 + 7.9953 X_4 + 0.0152 X_1 X_2 \\
& - 0.1258 X_1 X_3 + 0.0675 X_1 X_4 + 0.0034 X_2 X_3 \\
& - 0.0039 X_2 X_4 + 0.1253 X_3 X_4 - 5.2972 X_1^2 \\
& - 0.0018 X_2^2 - 0.1794 X_3^2 - 0.1277 X_4^2
\end{aligned} \tag{9}
$$

The ANOVA results for UAE (as shown in Tables 5 and S5–S7) revealed distinct significance patterns for extraction time (A), ultrasonic amplitude (B), solvent concentration (C), and temperature (D), highlighting their fundamental influence on mass transfer, cavitation intensity, and solvent–solute interactions. Solvent concentration (C) emerges as the most critical parameter, showing extremely high significance (p < 0.0001) for TPC, TFC, and AA due to EtOH's dual role in optimizing polyphenol solubility through polarity and enhancing cavitation induced cell disruption. Amplitude (B) exerts particularly strong effects on TFC (F = 37.63; p < 0.0001) and AA (F = 17.76; p = 0.0008) compared to TPC, reflecting that ultrasonic energy more

efficiently liberates bound flavonoids and influences antioxidant activity through cavitation intensity. Temperature (D) shows exceptional significance for AA ($p < 0.0001$) relative to TPC and TFC, highlighting the thermal sensitivity of antioxidant compounds that require precise temperature control to prevent degradation. Time (A), significant for all responses, demonstrates varying influence, most critical for AA ($p = 0.0062$) due to the kinetic requirements of antioxidant extraction, moderately important for TFC ($p = 0.0003$), and least influential for TPC ($p = 0.0031$). These differential significances are further evidenced by substantial quadratic terms, confirming nonlinear relationships between process parameters and extraction efficiency. The observed significance patterns are consistent with underlying physicochemical principles. Solvent exerted the strongest influence due to extraction thermodynamics, while amplitude enhanced bioactive compounds release through mechanical disruption; temperature affected antioxidant stability, and extraction time reflected compound-specific kinetic behavior. These findings highlight that solvent concentration and ultrasonic amplitude are critical for optimizing TFC and AA yields in UAE, whereas extraction time and temperature show minimal influence on TPC recovery. The second-order polynomial regression models—derived from the UAE process are shown in eqn (10)–(12).

$$
\begin{aligned}
Y_{(2,\text{TPC})} \text{ (mg GAE per g sample)} = &-626.0202 \\
&+ 5.6163A + 8.8415B + 8.7792C + 9.4641D \\
&+ 0.0611AB + 0.1112AC - 0.0353AD \\
&- 0.0072BC + 0.0055BD + 0.0074CD - 0.4750A^2 \\
&- 0.1246B^2 - 0.1049C^2 - 0.0936D^2
\end{aligned} \tag{10}
$$

$$
\begin{aligned}
Y_{(2,\text{TFC})} \text{ (mg QE per g sample)} = &-408.2041 \\
&+ 5.9028A + 5.5969B + 5.0305C + 5.7492D \\
&+ 0.0593AB + 0.0135AC + 0.0019AD \\
&- 0.0026BC - 0.0219BD + 0.0201CD \\
&- 0.3595A^2 - 0.0608B^2 - 0.0576C^2 - 0.0575D^2
\end{aligned} \tag{11}
$$

$$
\begin{aligned}
Y_{(2,\text{AA})} \text{ (\%)} = &-1128.2389 + 12.8208A + 16.8781B \\
&+ 13.1541C + 16.6926D + 0.3047AB \\
&+ 0.1600AC - 0.0370AD + 0.0311BC \\
&- 0.0911BD + 0.0558CD - 1.2574A^2 \\
&- 0.2127B^2 - 0.1809C^2 - 0.1482D^2
\end{aligned} \tag{12}
$$

MAE and UAE exhibited distinct interaction and quadratic effects, with variations in statistical significance highlighting differences in energy delivery mechanisms, mass transfer behavior, and solvent–solute interactions. In MAE, the extraction process was significantly influenced by the interaction between X_3 and X_4 ($p = 0.0219$). This interaction highlights the synergistic influence of thermal energy and solvent polarity, which together enhance polyphenol solubility and diffusion efficiency.[20,23] For TFC extraction, time exhibited significant interaction with solvent concentration ($X_1 \times X_3$, $p = 0.0226$) and temperature ($X_1 \times X_4$, $p = 0.0059$), indicating that extended exposure under optimal solvent and temperature conditions enhances flavonoid release *via* improved mass transfer.[18] For AA, the interaction between X_3 and X_4 ($p = 0.0030$) was the most

statistically significant, highlighting the importance of solvent polarity and precise temperature control in maximizing antioxidant yield while limiting oxidative degradation. Similarly, UAE demonstrated significant interaction effects between A and C ($p = 0.0034$ for TPC), indicating the role of solvent assisted cavitational disruption in enhancing polyphenol extraction.[10,29] For TFC, varied interactions were observed, including $A \times B$ ($p = 0.0152$), $B \times D$ ($p = 0.0235$), and $C \times D$ ($p = 0.0354$), reflecting the combined effect of solvent dynamics and acoustic cavitation intensity in flavonoid extraction. For AA, interaction between B and D ($p = 0.0089$) and A and B ($p = 0.0011$) highlighted the essential role of cavitation energy in enhancing antioxidant extraction while preventing oxidative losses.[24] Furthermore, highly significant quadratic effects ($p < 0.0001$) were observed for all process parameters in both MAE and UAE, indicating strong nonlinear relationships between independent variables and responses, with the exception of extraction time (X_1^2) in MAE for TPC. In MAE, the quadratic terms for microwave power (X_2^2), solvent concentration (X_3^2), and temperature (X_4^2) were highly significant ($p < 0.0001$), reflecting critical thresholds where dielectric heating and thermal degradation strongly influenced the extraction efficiency. However, the quadratic effect of time (X_1^2, $p = 0.0750$) on TPC was not statistically significant, suggesting a predominantly linear relationship with this parameter. Similarly, UAE showed dominant quadratic responses for all independent variables (A^2, B^2, C^2, and D^2, with $p < 0.0001$), highlighting the nonlinear effects of cavitation intensity, solvent polarity, and mass transfer on the extraction of target stevia metabolites.

3.2.2 Analysis of 3D response surface plots. Fig. 1–6 illustrate the quadratic relationships and factor interactions affecting TPC, TFC, and AA in both MAE and UAE processes. The curvature reveals optimal conditions and degradation thresholds, while contour distortions show parameter synergies, enabling comparative process optimization. During MAE, the obtained TPC, TFC, and AA in stevia leaf extract ranged from 55.73 ± 0.55 to 68.26 ± 0.43 mg GAE per g sample, 20.52 ± 0.11 to 31.97 ± 0.15 mg QE per g sample, and 61.33 ± 0.11 to $95.30 \pm 0.05\%$, respectively. Fig. 1(a–c) illustrates that TPC yield increases notably with microwave power, solvent concentration, and temperature, reaching optimal levels around 310 ± 20 W, $51 \pm 2\%$, and 51 ± 2 °C, respectively, at an extraction time of 5 ± 0.5 min. As shown in Table 4, the positive interaction coefficients between time and power ($\beta_{12} = +0.0104$) and time and solvent concentration ($\beta_{13} = +0.0941$) indicate synergistic effects that enhance TPC when these variables increase simultaneously. Fig. 1(d–e) illustrates the interaction of microwave power with solvent concentration and temperature, where the interaction between power and temperature ($\beta_{24} = +0.0002$) shows a negligible effect. However, the significant positive interaction between solvent concentration and temperature ($\beta_{34} = +0.0347$; $p = 0.0219$) in Fig. 1(f) suggests a combined enhancing effect on phenolic extraction. The non-significant quadratic effect of time (X_1^2; $p = 0.0750$) indicates a plateau in TPC near the optimal extraction time. Strong quadratic effects of temperature (X_4^2) and solvent concentration (X_3^2) ($p < 0.0001$) further emphasize the curvature in the response surface. TPC
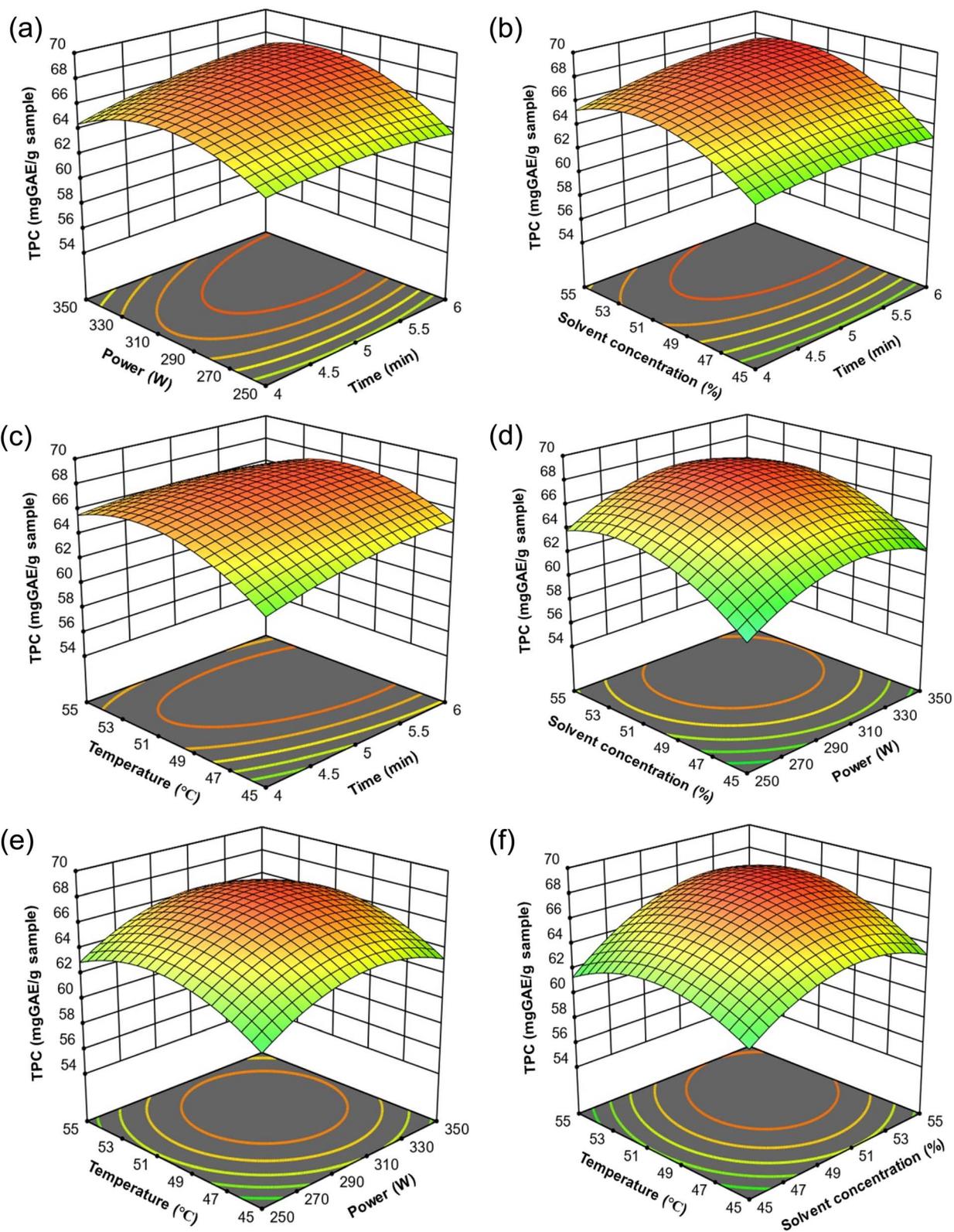
Fig. 1 Response surface methodology (RSM) plots for microwave assisted extraction (MAE) of total phenolic content (TPC) from stevia extract. The 3D response surface plots illustrate the effects of variable interactions on TPC yield: (a) power and time, (b) solvent concentration and time, (c) temperature and power, (d) solvent concentration and power, (e) temperature and time, and (f) temperature and solvent concentration.
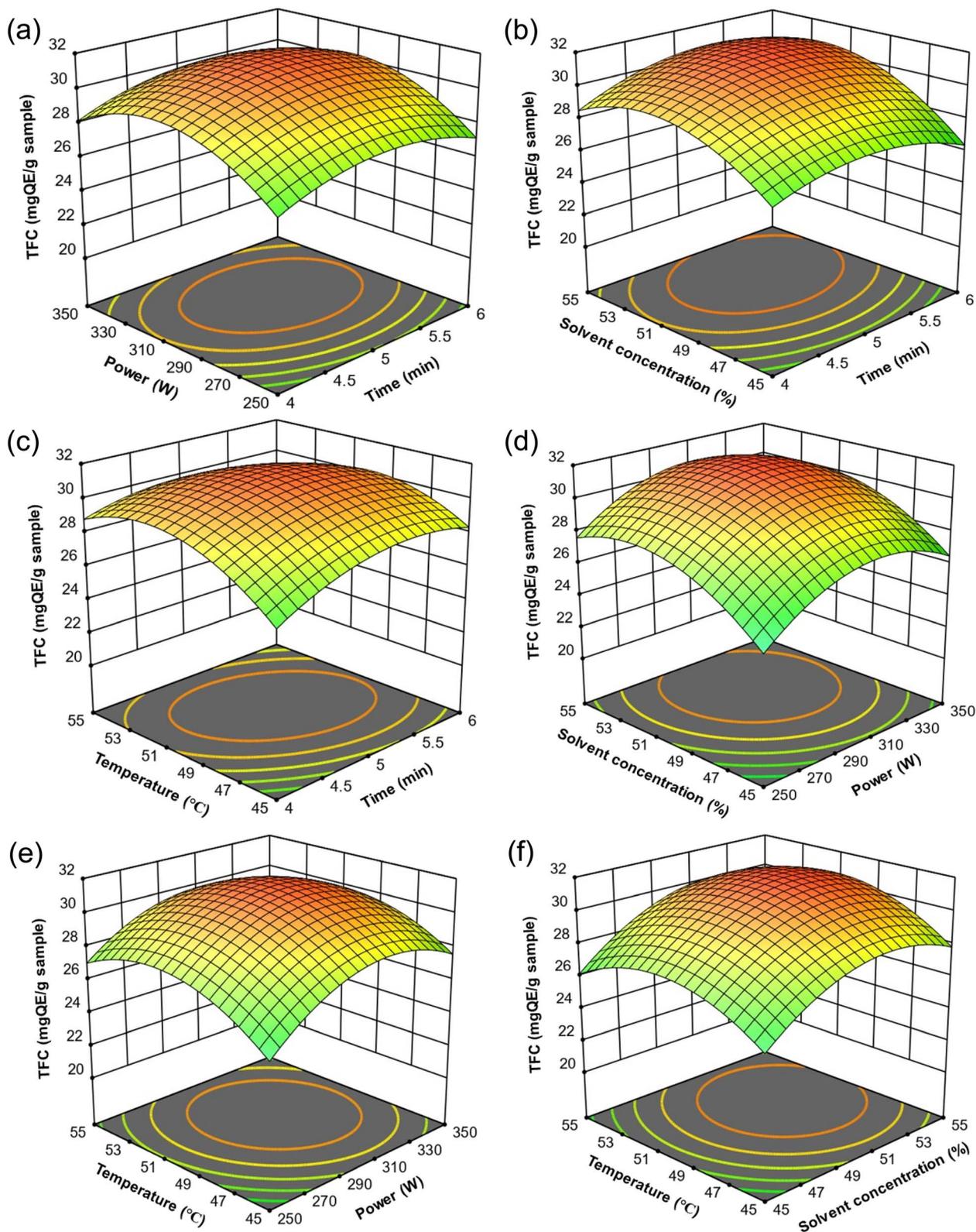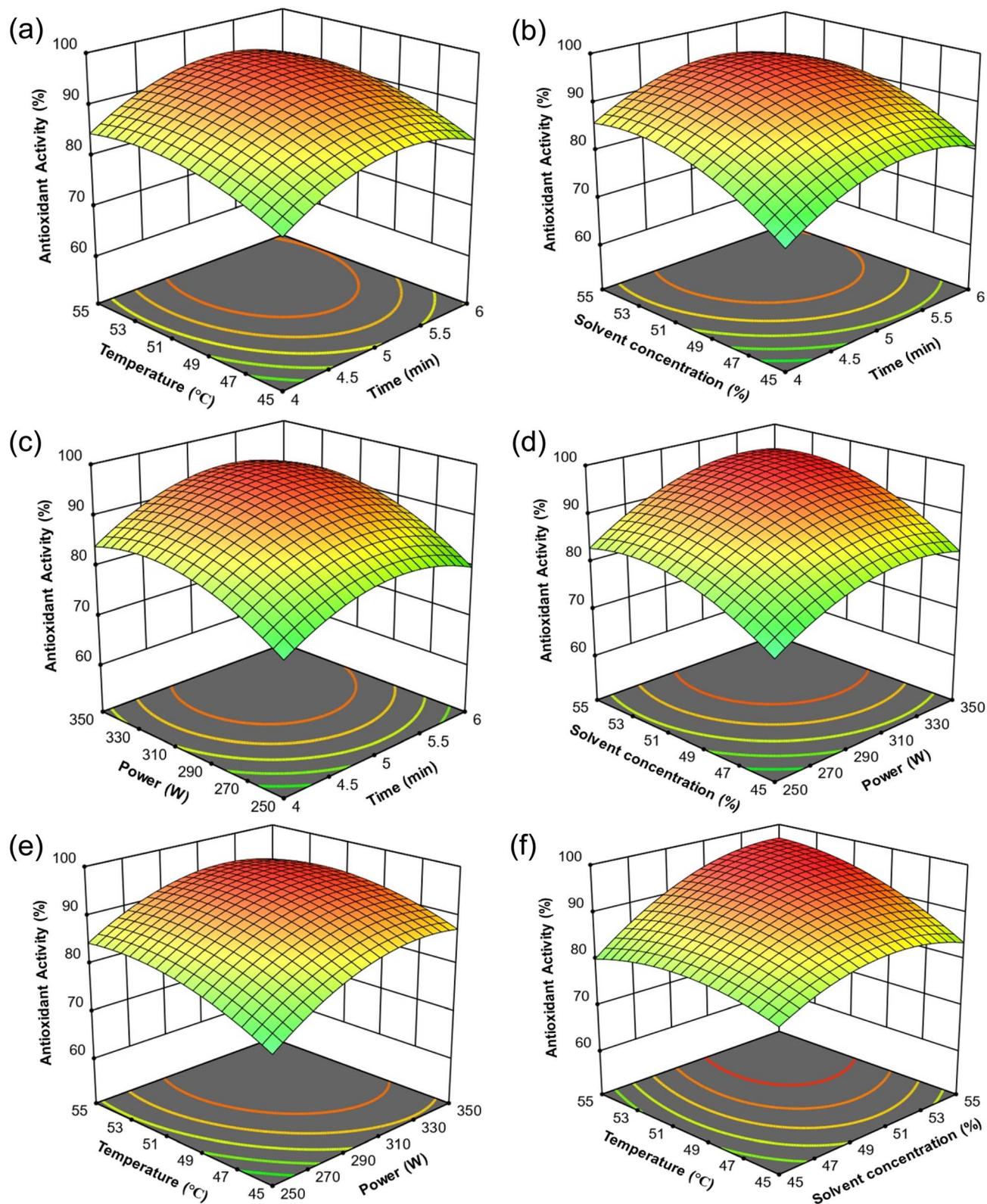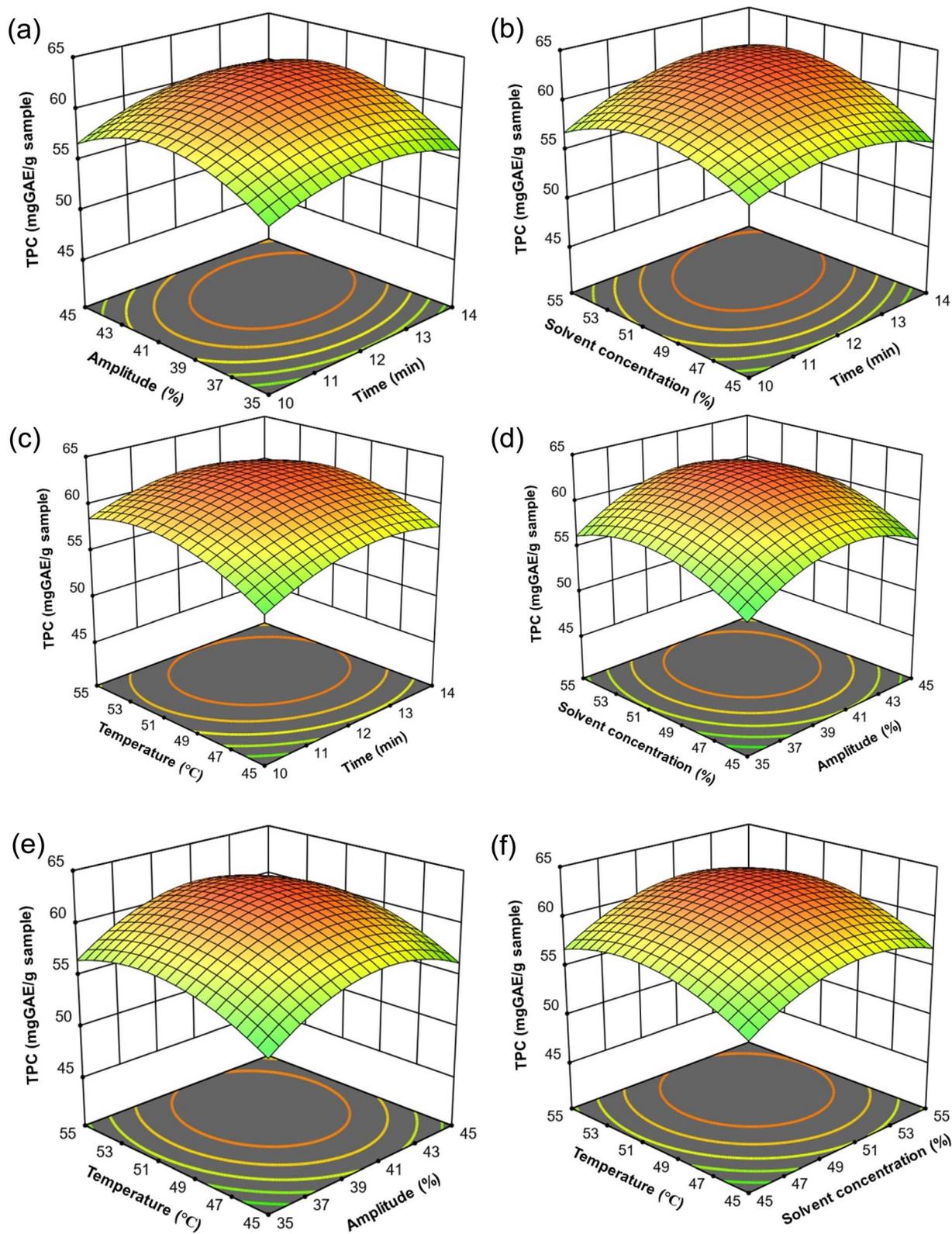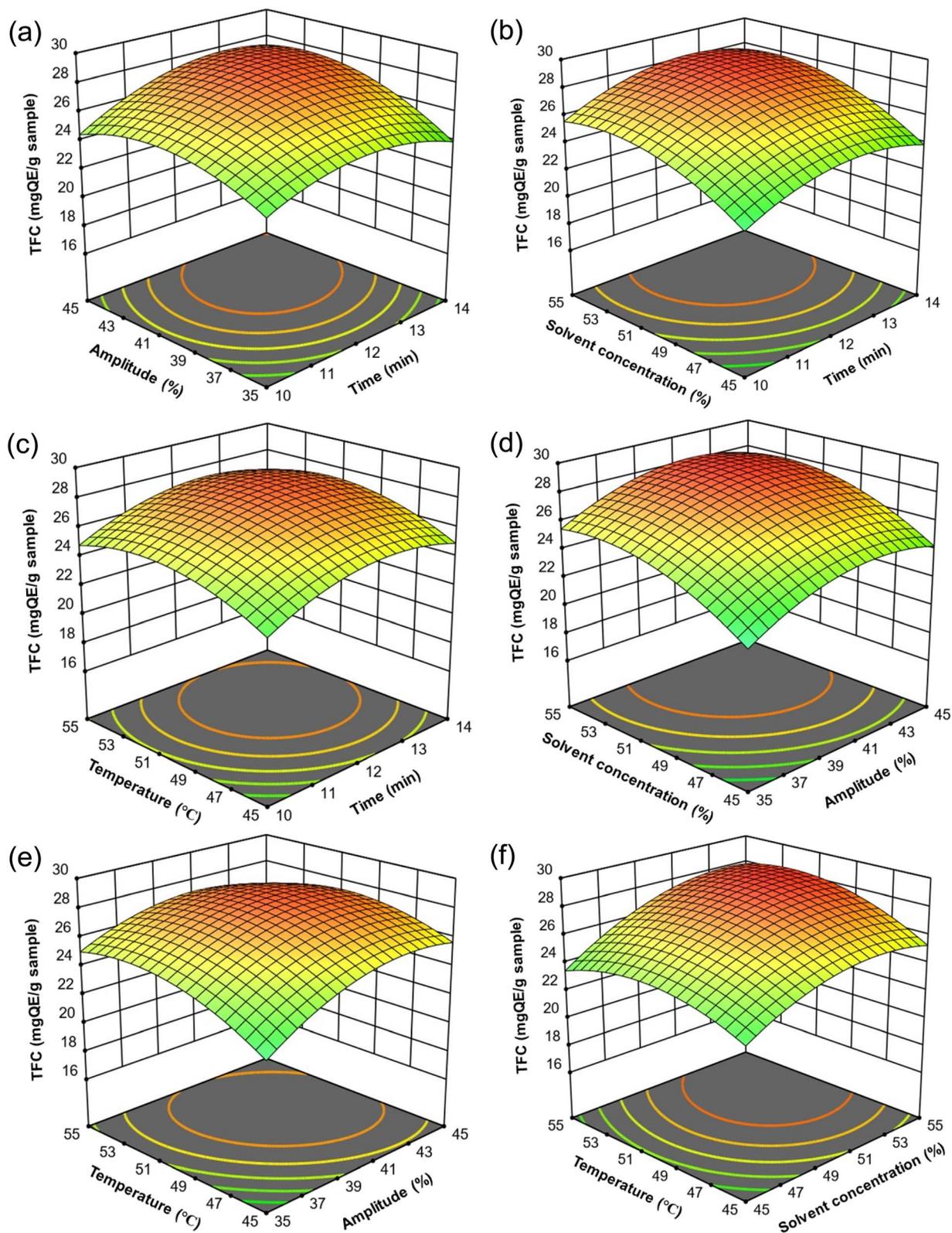
Fig. 2 Response surface methodology (RSM) plots demonstrating the impact of variable interactions on the extraction yield of total flavonoid content (TFC) from stevia using microwave assisted extraction (MAE). The 3D surface plots visualize the effects of paired variables: (a) microwave power and time, (b) solvent concentration and time, (c) temperature and time, (d) solvent concentration and power, (e) temperature and power, and (f) temperature and solvent concentration.

Fig. 3 Response surface methodology (RSM) plots depicting the effects of independent variables on the antioxidant activity (AA) yield during microwave assisted extraction (MAE) of stevia extract. The 3D response surfaces represent the interactions between variable pairs: (a) microwave power and extraction time, (b) solvent concentration and extraction time, (c) temperature and microwave power, (d) solvent concentration and microwave power, (e) temperature and extraction time, and (f) temperature and solvent concentration.

Fig. 4   Response surface methodology (RSM) plots for ultrasound assisted extraction (UAE) of total phenolic content (TPC) from stevia extract. The 3D response surface plots illustrate the effects of variable interactions on TPC yield: (a) amplitude and time, (b) solvent concentration and time, (c) temperature and amplitude, (d) solvent concentration and amplitude, (e) temperature and time, and (f) temperature and solvent concentration.
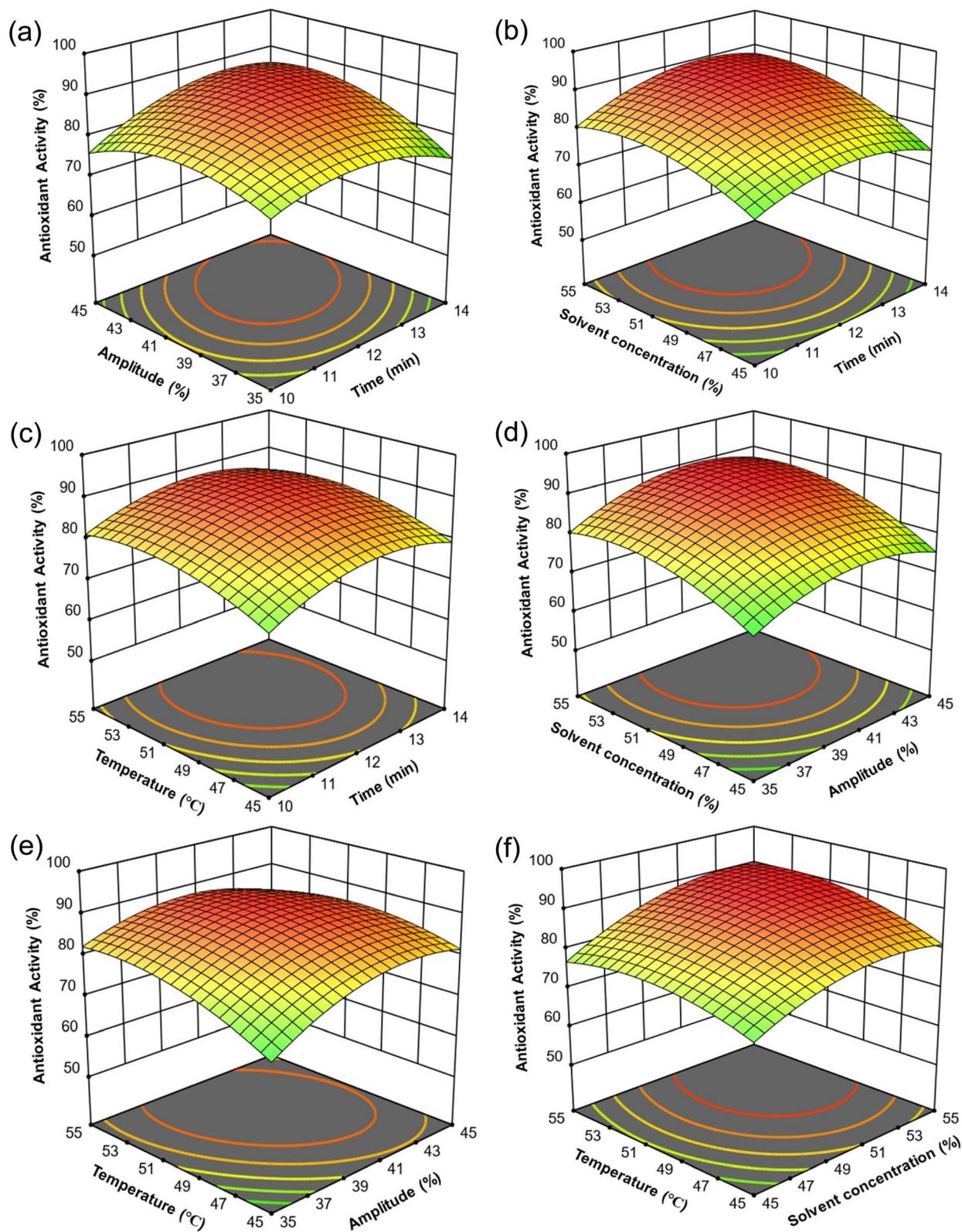
Fig. 5 Response surface methodology (RSM) plots demonstrating the impact of variable interactions on the extraction yield of total flavonoid content (TFC) from stevia using ultrasound assisted extraction (UAE). The 3D surface plots visualize the effects of paired variables: (a) amplitude and time, (b) solvent concentration and time, (c) temperature and time, (d) solvent concentration and amplitude, (e) temperature and amplitude, and (f) temperature and solvent concentration.

Fig. 6 Response surface methodology (RSM) plots depicting the effects of independent variables on the antioxidant activity (AA) yield during ultrasound assisted extraction (UAE) of stevia extract. The 3D response surfaces represent the interactions between variable pairs: (a) amplitude and extraction time, (b) solvent concentration and extraction time, (c) temperature and amplitude, (d) solvent concentration and amplitude, (e) temperature and extraction time, and (f) temperature and solvent concentration.

yield peaks around 51 ± 2 °C and $51 \pm 2\%$, beyond which thermal degradation likely reduces extraction efficiency. Similarly, surface plots for TFC extraction (Fig. 2(a–f)) reveal critical interactions between independent variables. In Fig. 2(a–c), excessive microwave power and prolonged extraction time resulted in the degradation of TFC, as indicated by the negative quadratic coefficients ($\beta_{11} = -1.1920$ and $\beta_{22} = -0.0008$, both with $p < 0.0001$). These curvature effects are likely associated with thermal or oxidative degradation occurring under intensified processing conditions. The positive and statistically significant interaction coefficient between extraction time and solvent concentration ($\beta_{13} = +0.0951$, $p = 0.0226$) indicates a synergistic effect, wherein simultaneous increases in both variables enhance the extraction of TFC. Fig. 2(d) demonstrates that beyond a threshold, higher solvent concentration does not improve extraction efficiency, even with increased microwave power, indicating solvent saturation effects. The interaction between temperature and microwave power in Fig. 2(e) further confirms that both factors contribute synergistically to TFC degradation. However, Fig. 2(f) highlights that balancing temperature and solvent concentration is essential for maximizing yield, as their combined effect exhibits a well-defined optimum. The 3D plots of antioxidant activity suggest that prolonged extraction time, high microwave power, elevated temperature, and excessive solvent concentration contribute to extract's antioxidant degradation, as shown in Fig. 3(a–f).

During UAE, the TPC, TFC, and AA in stevia leaf extract ranged from 46.10 ± 0.64 to 63.16 ± 1.58 mg GAE per g sample, 17.91 ± 0.16 to 28.71 ± 0.70 mg QE per g sample, and 54.47 ± 0.09 to $90.07 \pm 0.02\%$, respectively. The linear coefficients for time (A), ultrasonic amplitude (B), solvent concentration (C), and temperature (D) were highly significant ($p < 0.001$), except for time (A) in TPC ($p = 0.0031$) and AA ($p = 0.0062$), indicating their direct contribution to improving the initial extraction efficiency. The 3D response surface plots, along with significant negative quadratic coefficients ($p < 0.0001$, except for TPC) presented in Tables 4 and 5, confirmed a pronounced curvature effect. This indicates that moderate increases in extraction parameters enhance bioactive yield, whereas exceeding the optimal levels results in compound degradation. Fig. 4(a–f) highlights the optimal conditions for TPC extraction at around $41 \pm 2\%$ amplitude, $51 \pm 2\%$ solvent concentration, and 51 ± 2 °C temperature, with an extraction time of 12 ± 1 min. In TPC, the highly significant positive interaction between A and C ($\beta'_{13} = +0.1112$ with $p = 0.0034$) suggests that prolonged extraction enhances solvent effectiveness in dissolving phenolic compounds. Similarly, the 3D plots in Fig. 5(a–f) for TFC extraction exhibit comparable trends in response to the independent variables. The positive interaction between A and B ($\beta'_{12} = +0.0593$ with $p = 0.0154$) implies moderate synergy in flavonoid release with prolonged ultrasonication. However, the negative interaction between B and D ($\beta'_{24} = -0.0219$ with $p = 0.0235$) denotes flavonoid degradation under the combined effect of high ultrasonic amplitude and thermal stress. The positive $C \times D$ interaction ($\beta'_{34} = +0.0201$ with $p = 0.054$) suggests that increasing temperature within an optimal range improves flavonoid extraction. For AA (%), the 3D response

surface plots (Fig. 6 (a–f)) and statistical coefficients exhibit trends similar to TPC and TFC, characterized by a distinct curvature effect, as indicated by the significant negative
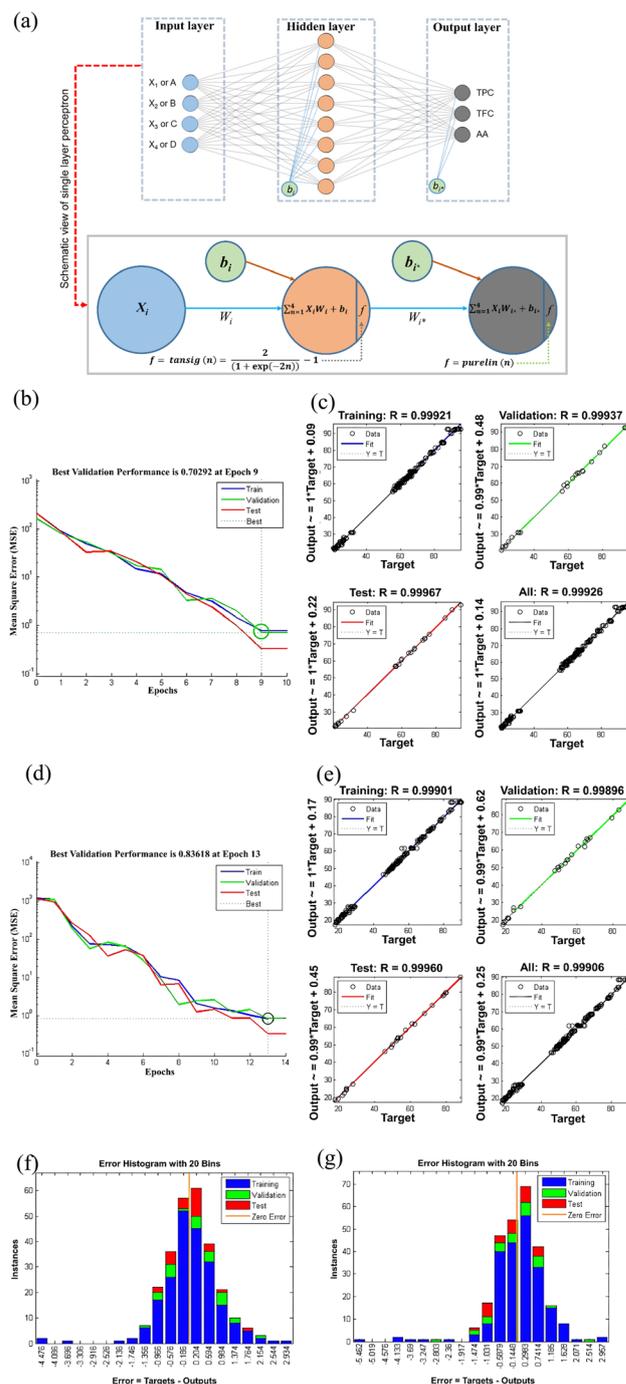

Fig. 7 (a) ANN architecture illustrating the layer configuration and connectivity with schematic diagram of single perceptron, (b) training, validation, and test performance curves showing the mean squared error (MSE) over epochs for the MAE dataset, with the best validation performance. (c) Regression plots for MAE, showing the relationship between predicted and actual values along with the correlation coefficient (R). (d) Validation MSE curve for the UAE dataset. (e) Regression plots for UAE predictions. (f and g) Error histograms (20 bins) for MAE and UAE, illustrating the distribution of prediction errors across training, validation, and test datasets.

quadratic terms for A^2, B^2, C^2, and D^2 ($p < 0.0001$). The positive interaction between A and B ($\beta'_{12} = +0.3047$ with $p = 0.0011$) indicates that moderate increases in both parameters enhance antioxidant activity; however, excessive ultrasonication may trigger oxidative degradation, reducing overall extraction efficiency.

The comparative analysis between MAE and UAE demonstrated that MAE exhibited enhanced extraction efficiency, with the highest experimental TPC, TFC, and AA values increasing by 8.07%, 11.34%, and 5.82%, respectively, compared to those obtained with UAE. The enhanced extraction efficiency observed with MAE was achieved with 58.33% less extraction time. This can be attributed to its rapid volumetric heating mechanism. This mechanism promotes a more uniform distribution of thermal energy throughout the sample matrix, which in turn facilitates efficient cell wall disruption and subsequent compound diffusion. However, UAE's dependence on transient cavitation phenomena resulted in localized energy hotspots and uneven compound extraction. Furthermore, prolonged ultrasonication duration in UAE likely induced thermal degradation of thermolabile secondary metabolites, as evidenced by the comparatively lower yields of bioactive compounds.[12,20,23,26,37]

3.3 ANN model analysis

A systematic evaluation of hidden layer configurations was performed to develop optimized ANN models for both MAE and UAE techniques. Among the tested architectures (7–10 neurons), the 8-neuron hidden layer model (Fig. 7(a)) demonstrated superior performance for both methods. For MAE, the lowest mean squared error (MSE = 0.7029) was achieved at epoch 9 with a high R^2 of 0.9985, indicating strong predictive accuracy and fast convergence. In comparison, UAE showed a slightly higher MSE of 0.8362 at epoch 13 with a lower R^2 of 0.9981. The training performance of the MAE model (Fig. 7(b)) showed well-aligned and smooth curves for training, validation, and testing datasets, reflecting effective learning with minimal overfitting. Whereas, the UAE model (Fig. 7(d)) showed greater fluctuations, particularly in the validation and test phases, suggesting unstable learning and potential overfitting.

Regression plots (Fig. 7(c) and (e)) further confirmed the better predictive performance of the MAE model, as shown by higher regression coefficients and tighter data fitting. The final ANN model architecture employed L2 regularization ($\lambda = 0.12$), the Levenberg–Marquardt training algorithm for efficient gradient-based optimization, and a hybrid genetic algorithm for fine-tuning hyperparameters. The use of the tansig activation function in the hidden layer and the purelin function in the output layer facilitated effective nonlinear transformation and output scaling with a network topology of 4-8-3. Fig. 7(f–g) presents the error histograms with 20 bins for the MAE and UAE models. In both cases, the majority of errors are densely concentrated around zero, indicating high prediction accuracy and minimal bias. The maximum observed errors were approximately +2.93 for MAE and +2.96 for UAE, reflecting the models' low error tendency and overall reliability. Overall, the ANN model developed for MAE demonstrated greater robustness, precision, and generalization capability compared to that for UAE.

3.4 Comparison of the developed RSM and ANN models

The predictive performance of RSM and ANN models for both MAE and UAE techniques was assessed using statistical metrics including MSE, RMSE, MAD, MAPE, R^2, and adjusted R^2 as presented in Table 6. For all responses (TPC, TFC, and AA), the ANN models consistently outperformed the RSM models, as evidenced by lower error values and higher adjusted R^2. Specifically, the adjusted R^2 values ranged from 0.9421 to 0.9832 for MAE and from 0.9499 to 0.9861 for UAE, confirming superior prediction accuracy and reliability.

3.5 RSM and ANN model prediction and validation

Optimization of secondary metabolite extraction from stevia was carried out using both RSM and ANN models, as presented in Table 7. For MAE, RSM identified optimal conditions as an extraction time (X_1) of 4.31 min, a microwave power (X_2) of 312.50 W, an ethanol concentration (X_3) of 52.41%, and a temperature (X_4) of 52.10 °C. This model predicted maximum yields of 67.10 mg GAE per g sample for $Y_{(1,TPC)}$, 30.32 mg QE per g sample for $Y_{(1,TFC)}$, and 91.89% antioxidant inhibition for $Y_{(1,AA)}$, with a desirability score of 0.879. In comparison, the

Table 6 Statistical evaluation of experimental and predicted responses from RSM and ANN models[a]

	MAE						UAE					
	TPC		TFC		AA		TPC		TFC		AA	
Performance metrics	RSM	ANN	RSM	ANN	RSM	ANN	RSM	ANN	RSM	ANN	RSM	ANN
MSE	0.9189	0.4753	0.2794	0.4329	6.2974	1.0733	0.8189	0.2591	0.3783	0.2744	4.5946	0.7757
RMSE	0.9586	0.6895	0.5219	0.6580	2.5095	1.0366	0.9049	0.5090	0.61509	0.5238	2.1435	0.8807
MAD	0.8303	0.5568	0.4536	0.5388	2.0413	0.5875	0.7243	0.3694	0.5197	0.4604	1.7627	0.5016
MAPE	1.3169	0.8929	1.7675	2.1246	2.4711	0.6870	1.3633	0.6506	2.2106	1.9677	2.3294	0.6082
R^2	0.9428	0.9700	0.9758	0.9840	0.9480	0.9913	0.9651	0.9889	0.9643	0.9741	0.9574	0.9928
Adjusted R^2	0.8893	0.9421	0.9528	0.9691	0.8994	0.9832	0.9325	0.9786	0.9309	0.9499	0.9177	0.9861

[a] Here, MSE: mean squared error, RMSE: root mean squared error, MAD: mean absolute deviation, MAPE: mean absolute percentage error, MAE: microwave assisted extraction, UAE: ultrasound assisted extraction, TPC: total phenolic content, TFC: total flavonoid content, AA: antioxidant activity, RSM: response surface methodology, and ANN: artificial neural network.

Table 7 Experimental validation and percentage error comparison of RSM and ANN model predictions for TPC, TFC, and AA under optimal MAE and UAE conditions[a]

Parameter	Model optimization				Experimental validation							
	MAE (RSM)	MAE (ANN–GA)	UAE (RSM)	UAE (ANN–GA)	MAE (RSM)	MAE (ANN–GA)	UAE* (RSM)	UAE* (ANN–GA)	MAE (RSM) Error (%)	MAE (ANN) Error (%)	UAE (RSM) Error (%)	UAE (ANN) Error (%)
	Optimal conditions				**Optimal conditions for experimentation**							
Time (min)	4.31 min	5.15 min	10.90 min	13.25 min	4.31 min	5.15 min	11.00 min	13.00 min	—	—	—	—
Microwave power (W) or ultrasound amplitude (%)	312.50 W	284.05 W	40.62%	41.25%	312.50 W	284.05 W	41.00%	41.00%	—	—	—	—
Solvent concentration (%)	52.41%	53.10%	52.15%	52.71%	52.41%	53.10%	52.00%	53.00%	—	—	—	—
Temperature (°C)	52.10 °C	53.89 °C	51.87 °C	50.36 °C	52.10 °C	53.89 °C	52.00 °C	50.00 °C	—	—	—	—
	Predicted values				**Experimental values**				Error (%)		Error (%)	
TPC (mg GAE per g sample)	67.10	67.53	61.14	62.37	65.12 ± 0.35	68.25 ± 0.20	59.77 ± 0.53	62.81 ± 0.59	3.04	1.05	2.29	0.70
TFC (mg QE per g sample)	30.32	29.80	27.52	28.96	28.22 ± 0.26	29.90 ± 0.19	25.15 ± 0.27	28.59 ± 0.47	7.43	0.32	9.44	1.32
AA (%)	91.89	96.34	87.89	92.33	87.28 ± 0.37	95.98 ± 0.39	85.04 ± 0.46	91.40 ± 0.49	5.29	0.48	3.35	1.01

[a] Here, TPC represents the total phenolic content (mg GAE per g sample), TFC denotes the total flavonoid content (mg QE per g sample), and AA denotes the antioxidant activity or inhibition (%). QE refers to quercetin equivalent, GAE signifies gallic acid equivalent, MAE represents microwave assisted extraction, UAE denotes ultrasound assisted extraction, ANN stands for the artificial neural network, GA stands for the genetic algorithm, and RSM represents the response surface methodology. *Model-predicted values for UAE conditions were rounded off (shown in bold) due to instrument decimal constraints.

RSM model for UAE required a longer extraction time of 10.90 min, 40.62% ultrasonic amplitude, 52.15% ethanol concentration, and a temperature of 51.87 °C, predicting lower yields of 61.14 mg GAE per g sample for $Y_{(2,\text{TPC})}$, 27.52 mg QE per g sample for $Y_{(2,\text{TFC})}$, and 87.89% antioxidant inhibition for $Y_{(2,\text{AA})}$, with a desirability score of 0.867. During this RSM-based desirability function approach, extraction time was assigned a minimization weight, while the responses were targeted for maximization. To further fine-tune these conditions, an ANN model combined with GA was utilized. The ANN-GA approach predicted optimal conditions for MAE as 5.15 min, 284.05 W, 53.10% ethanol concentration, and 53.89 °C, estimating yields of 67.53 mg GAE per g sample (TPC), 29.80 mg QE per g sample (TFC), and 96.34% antioxidant inhibition (AA). For UAE, the optimized parameters were 13.25 min, 41.25% ultrasonic amplitude, 52.71% ethanol concentration, and 50.36 °C, with predicted yields of 62.37 mg GAE per g sample (TPC), 28.96 mg QE per g sample (TFC), and 92.33% of antioxidant inhibition (AA). The ANN model demonstrated robust optimization, converging after 87 generations for MAE and 96 generations for UAE.

Previous studies have shown that phenolic extraction from stevia varies significantly based on the extraction method and process parameters. For instance, Yilmaz et al.[34] reported a TPC yield of 67.8 mg GAE per g sample using MAE at 16 min and 51 °C, while UAE required 43 min at 50 °C to obtain a comparable value of 68.6 mg GAE per g sample. Similarly, Kaur et al.[38] found 28.59–32.44 mg GAE per g sample of TPC with 53.57–62.39% inhibition of DPPH free radicals using UAE (50% ethanol concentration, 50 °C, and 30 min). Ameer et al.[39] however, reported only 25.76 mg GAE per g sample of TPC under supercritical fluid extraction (40% ethanol concentration, 45 °C, and 225 bar). Zaidan et al.[13] found ethanolic extraction values of 6.65 mg GAE per g sample of TPC and 10.91 mg QE per g sample of TFC (1 : 10 g mL^{-1}, 40 °C, 200 rpm for 90 min), and Ali et al.[40] found a maximum TPC of 41.00 ± 0.69 mg GAE per g sample and a TFC of 22.66 ± 0.04 mg QE per g sample using maceration (1 : 10 g mL^{-1}, 50% methanol concentration, 200 rpm for 60 min).

During experimental validation, the ANN–GA optimized MAE and UAE processes in the present study exhibited higher extraction efficiency and significant time savings compared to previously reported results. The optimized MAE (ANN–GA) process yielded 68.25 mg GAE per g sample for TPC, 29.90 mg QE per g sample for TFC, and 95.98% of antioxidant inhibition (AA) in just 5.15 min. In comparison, the optimized UAE (ANN–GA) process achieved slightly lower yields of 62.81 mg GAE per g sample for TPC, 28.59 mg QE per g sample for TFC, and 91.40% antioxidant inhibition (AA) over a longer duration of 13 min. Furthermore, the optimized values predicted by the ANN–GA model for both MAE and UAE showed excellent agreement with experimental results and outperformed the RSM model, with relative percentage errors below 1.32% (as shown in Table 7). Although the TPC values were comparable to those reported by Yilmaz et al.[34] (67.8–68.6 mg GAE per g sample), the optimized process in the present study achieved the same recovery with 67.81% and 69.77% shorter extraction time for MAE and UAE, respectively. In comparison with Kaur et al.[38] the optimized UAE process achieved 1.94–2.20 times higher TPC recovery with

46.49–70.62% greater antioxidant activity, while reducing the extraction time by 56.67%. Furthermore, compared to the yield reported by Zaidan et al.[13] the present study's findings for TPC and TFC were 9.44–10.27 times and 2.62–2.74 times higher, respectively. Similarly, when compared to the results of Ali et al.[40] the TPC and TFC values were 1.53–1.66 times and 1.26–1.32 times higher, respectively. Moreover, the ANN–GA optimized MAE process demonstrated enhanced extraction efficiency with moderate power input, reduced solvent consumption, shorter extraction time, and efficient energy utilization. Collectively, these outcomes establish MAE as a sustainable, time-efficient, and highly effective approach for the recovery of phenolics and related bioactive compounds from *Stevia rebaudiana*.

4 Conclusion

Secondary bioactive compounds from *Stevia rebaudiana* are well-known for their health-promoting properties, including anti-inflammatory and antioxidant effects. This study aimed to optimize MAE and UAE conditions using RSM and ANN–GA. The findings revealed that MAE outperformed UAE under optimized conditions, yielding a higher TPC of 65.12 ± 0.35 mg GAE per g sample, a TFC of 28.22 ± 0.26 mg QE per g sample, and an AA of $87.28 \pm 0.37\%$, compared to UAE's TPC of 59.77 ± 0.53 mg GAE per g sample, TFC of 25.15 ± 0.27 mg QE per g, and AA of $85.04 \pm 0.46\%$. MAE demonstrated an improvement of 8.95% in TPC, 12.21% in TFC, and 2.63% in AA over UAE while also reducing the extraction time by 67.47%. The predicted R^2 values from RSM (0.7048–0.8971 for MAE and 0.7813–0.8276 for UAE) indicated limitations in predictive accuracy, prompting the adoption of an ANN–GA approach for enhanced model performance and optimization. The ANN–GA model showed superior predictive accuracy, with predicted values closely matching experimental results and exhibiting lower errors than RSM. Using ANN–GA, the optimized MAE conditions were determined to be an extraction time of 5.15 min, a microwave power of 284.05 W, an ethanol concentration of 53.10%, and a temperature of 53.89 °C. Under these conditions, the extraction yielded 68.25 ± 0.20 mg GAE per g sample TPC, 29.90 ± 0.19 mg QE per g sample TFC, and $95.98 \pm 0.39\%$ AA. Compared to UAE under ANN–GA optimization, MAE achieved an increase of 8.66% in TPC, 4.60% in TFC, and 5.01% in AA while demonstrating greater energy efficiency and a 60.38% reduction in extraction time. These findings establish MAE as a more sustainable and effective method for extracting bioactive compounds from medicinal plants in general, offering significant advantages over UAE in terms of both yield and environmental impact.

Nomenclature

Symbols

3D	Three dimensional
A	Extraction time (min) for UAE
B	Ultrasonic amplitude (%) for UAE
C	Solvent concentration (%) for UAE
D	Temperature (°C) for UAE
DPPH	2,2-Diphenyl-2-picrylhydrazyl
N	Number of experimental runs
R	Correlation coefficient
R^2	Coefficient of determination
$X1$	Extraction time (min) for MAE
$X2$	Microwave power (W) for MAE
$X3$	Solvent concentration (%) for MAE
$X4$	Temperature (°C) for MAE
$Y_{\exp,i}$	Experimental value of the ith term
$\bar{Y}_{\exp,i}$	Mean experimental value of the ith term
$\hat{Y}_{\text{pre},i}$	Predicted value of the ith term

Abbreviations

AA	Antioxidant activity (%)
ANN	Artificial neural network
ANN–GA	Artificial neural network coupled with genetic algorithm
CCRD	Central composite rotatable design
FCR	Folin–Ciocalteu reagent
GA	Genetic algorithm
GAE	Gallic acid equivalent
MAE	Microwave assisted extraction
MAPE	Mean absolute percentage error
MSE	Mean squared error
QE	Quercetin equivalent
RMSE	Root mean squared error
SFAT	Single factor at a time
TFC	Total flavonoid content (mg QE per g sample)
TPC	Total phenolic content (mg GAE per g sample)
UAE	Ultrasound assisted extraction

Author contributions

Prakash Kumar: conceptualization, methodology, software, data curation, validation, formal analysis, visualization, and writing – original draft. Punyadarshini Punam Tripathy (P. P. Tripathy): conceptualization, methodology, investigation, visualization, supervision, validation, funding acquisition, resources, writing – reviewing & editing.

Conflicts of interest

The authors declare no competing interests.

Data availability

Data will be made available on request.

Supplementary information is available. See DOI: **https://doi.org/10.1039/d5fb00329f**.

Acknowledgements

References

1 J. Wang, H. Zhao, Y. Wang, H. Lau, W. Zhou, C. Chen and S. Tan, *Trends Food Sci. Technol.*, 2020, **103**, 264–281, DOI: 10.1016/j.tifs.2020.07.023.

2 M. Sevindik, A. Gürgen, T. Krupodorova, İ. Uysal and O. Koçer, *Sci. Rep.*, 2024, **14**, 31403, DOI: 10.1038/s41598-024-83029-8.

3 B. S. Patil, G. K. Jayaprakasha, K. N. Chidambara Murthy and A. Vikram, *J. Agric. Food Chem.*, 2009, **57**(18), 8142–8160, DOI: 10.1021/jf9000132.

4 A. M. Pisoschi, A. Pop, F. Iordache, L. Stanca, G. Predoi and A. I. Serban, *Eur. J. Med. Chem.*, 2021, **209**, 112891, DOI: 10.1016/j.ejmech.2020.112891.

5 A. K. Jha and N. Sit, *Trends Food Sci. Technol.*, 2022, **119**, 579–591, DOI: 10.1016/j.tifs.2021.11.019.

6 V. Chatsudthipong and C. Muanprasat, *Pharmacol. Ther.*, 2009, **121**(1), 41–54, DOI: 10.1016/j.pharmthera.2008.09.007.

7 K. zar Myint, K. Wu, Y. Xia, Y. Fan, J. Shen, P. Zhang and J. Gu, *J. Food Sci.*, 2020, **85**(2), 240–248, DOI: 10.1111/1750-3841.15017.

8 R. Lemus-Mondaca, A. Vega-Gálvez, L. Zura-Bravo and A. H. Kong, *Food Chem.*, 2012, **132**(3), 321–328, DOI: 10.1016/j.foodchem.2011.11.140.

9 P. Kumar, P. Rani and P. P. Tripathy, *Biomass Convers. Biorefin.*, 2025, **15**, 7523–7542, DOI: 10.1007/s13399-024-05725-9.

10 A. G. Covarrubias-Cárdenas, J. I. Martínez-Castillo, N. Medina-Torres, T. Ayora-Talavera, H. Espinosa-Andrews, N. U. García-Cruz and N. Pacheco, *Agronomy*, 2018, **8**(9), 170, DOI: 10.3390/agronomy8090170.

11 T. F. O. da Silva, A. A. Ferrarezi, É. da Silva Santos, S. T. C. Ribeiro, A. J. B. de Oliveira and R. A. C. Gonçalves, *Food Sci. Biotechnol.*, 2025, **34**, 1679–1697, DOI: 10.1007/s10068-024-01776-w.

12 D. T. Raspe, C. da Silva and S. Cláudio da Costa, *Food Biosci.*, 2022, **46**, 101593, DOI: 10.1016/j.fbio.2022.101593.

13 U. H. Zaidan, N. I. Mohamad Zen, N. A. Amran, S. Shamsi and S. S. A. Gani, *Biocatal. Agric. Biotechnol.*, 2019, **18**, 101049, DOI: 10.1016/j.bcab.2019.101049.

14 E. Yildiz-Ozturk, A. Nalbantsoy, O. Tag and O. Yesil-Celiktas, *Ind. Crops Prod.*, 2015, **77**, 961–971, DOI: 10.1016/j.indcrop.2015.10.010.

15 C. Boonkaewwan and A. Burodom, *J. Sci. Food Agric.*, 2013, **93**(15), 3820–3825, DOI: 10.1002/jsfa.6287.

16 J. Wang, Q. Li, Z. Chen, X. Qi, X. Wu, G. Di, J. Fan and C. Guo, *Toxicol. Appl. Pharmacol.*, 2021, **419**, 115511, DOI: 10.1016/j.taap.2021.115511.

17 R. Lemus-Mondaca, A. Vega-Gálvez, P. Rojas, K. Stucken, C. Delporte, G. Valenzuela-Barra, R. J. Jagus, M. V. Agüero and A. Pasten, *J. Appl. Res. Med. Aromat. Plants*, 2018, **11**, 37–46, DOI: 10.1016/j.jarmap.2018.10.003.

18 Y. A. Bhadange, J. Carpenter and V. K. Saharan, *ACS Omega*, 2024, **9**(29), 31274–31297, DOI: 10.1021/acsomega.4c02718.

19 J. Azmir, I. S. M. Zaidul, M. M. Rahman, K. M. Sharif, A. Mohamed, F. Sahena, M. H. A. Jahurul, K. Ghafoor, N. A. N. Norulaini and A. K. M. Omar, *J. Food Eng.*, 2013, **117**(4), 426–436, DOI: 10.1016/j.jfoodeng.2013.01.014.

20 I. S. Che Sulaiman, M. Basri, H. R. Fard Masoumi, W. J. Chee, S. E. Ashari and M. Ismail, *Chem. Cent. J.*, 2017, **11**(54), DOI: 10.1186/s13065-017-0285-1.

21 L. Meena, N. N. Gowda, C. K. Sunil, A. Rawson and S. Janghu, *J. Food Compos. Anal.*, 2024, **126**, 105899, DOI: 10.1016/j.jfca.2023.105899.

22 A. A. Bin Mokaizh, A. H. Nour and K. Kerboua, *Ultrason. Sonochem.*, 2024, **105**, 106852, DOI: 10.1016/j.ultsonch.2024.106852.

23 G. Dip, P. Aggarwal, A. Kapoor, S. Grover and S. Kaur, *Biomass Bioenergy*, 2025, **195**, 107709, DOI: 10.1016/j.biombioe.2025.107709.

24 S. K. Bhangu and M. Ashokkumar, in *Sonochemistry: From Basic Principles to Innovative Applications*, ed. J. C. Colmenares and G. Chatel, Springer, Cham, 2017, pp. 1–28, DOI: 10.1007/s41061-016-0054-y.

25 A. Periche, M. L. Castelló, A. Heredia and I. Escriche, *Plant Foods Hum. Nutr.*, 2015, **70**, 119–127, DOI: 10.1007/s11130-015-0475-8.

26 K. Ameer, S. W. Bae, Y. Jo, H. G. Lee, A. Ameer and J. H. Kwon, *Food Chem.*, 2017, **229**, 198–207, DOI: 10.1016/j.foodchem.2017.01.121.

27 K. Ameer, S. Ameer, Y. M. Kim, M. Nadeem, M. K. Park, M. A. Murtaza, M. A. Khan, M. A. Nasir, G. Mueen-Ud-din, S. Mahmood, T. Kausar and M. Abubakar, *Foods*, 2022, **11**(6), 883, DOI: 10.3390/foods11060883.

28 A. Javed, M. Naznin, M. B. Alam, A. Fanar, B. R. Song, S. Kim and S. H. Lee, *Antioxidants*, 2022, **11**(11), 2246, DOI: 10.3390/antiox11112246.

29 D.-Z. Jiang, D.-P. Yu, M. Zeng, W.-B. Liu, D.-L. Li and K.-Y. Liu, *RSC Adv.*, 2024, **14**, 39069–39080, DOI: 10.1039/D4RA05077K.

30 P. Kumar and P. P. Tripathy, *J. Food Process. Eng.*, 2024, **47**(12), e14760, DOI: 10.1111/jfpe.14760.

31 A. Ali, R. Shahu, P. Balyan, S. Kumari, R. Ghodmare, R. Jobby and P. Jha, *Sugar Technol.*, 2022, **24**, 563–575, DOI: 10.1007/s12355-021-01023-0.

32 J. M. Carbonell-Capella, J. Šic Žlabur, S. Rimac Brnčić, F. J. Barba, N. Grimi, M. Koubaa, M. Brnčić and E. Vorobiev, *J. Food Process. Preserv.*, 2017, **41**(5), e13179, DOI: 10.1111/jfpp.13179.

33 A. Antony and M. Farid, *Appl. Sci.*, 2022, **12**(4), 2107, DOI: 10.3390/app12042107.

34 F. M. Yilmaz, A. Görgüç, Ö. Uygun and C. Bircan, *Separ. Sci. Technol.*, 2021, **56**(11), 936–948, DOI: 10.1080/01496395.2020.1743311.

35 O. A. Olalere and C. Y. Gan, *Separ. Sci. Technol.*, 2021, **56**, 1853–1865, DOI: 10.1080/01496395.2020.1795678.

36 I. D. Boateng, *Food Bioprocess Technol.*, 2024, **17**, 1109–1140, DOI: 10.1007/s11947-023-03171-5.

37 A. A. Bin Mokaizh, A. Hamid Nour, G. A. M. Ali, C. Ishmael Ukaegbu and E. Faraj Hawege, *J. Ind. Eng. Chem.*, 2025, **142**, 321–328, DOI: **10.1016/j.jiec.2024.07.038**.

38 R. Kaur, P. Manchanda and G. S. Sidhu, *J. Food Meas. Char.*, 2022, **16**, 461–470, DOI: **10.1007/s11694-021-01176-2**.

39 K. Ameer, B. S. Chun and J. H. Kwon, *Ind. Crops Prod.*, 2017, **109**, 672–685, DOI: **10.1016/j.indcrop.2017.09.023**.

40 A. Ali, R. Shahu, P. Balyan, S. Kumari, R. Ghodmare, R. Jobby and P. Jha, *Sugar Technol.*, 2022, **24**, 563–575, DOI: **10.1007/s12355-021-01023-0**.